1986

State modeling of clock noises and its application

In Soo Ahn
Iowa State University

Ahn, In Soo

STATE MODELING OF CLOCK NOISES AND ITS APPLICATION

Iowa State University PH.D. 1986

State modeling of clock noises and its application

by

In Soo Ahn

A Dissertation Submitted to the

Graduate Faculty in Partial Fulfillment of the

Requirements for the Degree of

DOCTOR OF PHILOSOPHY

Department: Electrical Engineering and Computer Engineering
Major: Electrical Engineering (Control System)

Approved:

Signature was redacted for privacy.

In Charge of Major Work

Signature was redacted for privacy.

For the Major Department

Signature was redacted for privacy.

For the Graduate College

Iowa State University
Ames, Iowa

1986

TABLE OF CONTENTS

LIST OF TABLES

LIST OF FIGURES

I. INTRODUCTION TO THE CLOCK NOISE MODELING

A. Introduction

Precision time keeping is important for daily life and most branches of science. In order to keep the time accurate, a stable oscillator is necessary. An atomic or a quartz crystal clock is used to generate highly stable clock pulses. Particularly, the atomic clock is used as a primary source for the time standard.

Since the time is derived from counting clock pulses or measuring frequencies, timing accuracy is directly related to the fluctuations in oscillator frequency. Frequency fluctuation has many causes. Among them, some are known and some unknown. Largely, these causes can be divided into two categories. First, it is influenced to some extent by its environment, i.e., changes in ambient temperature, humidity, vibration, acceleration, radiation, pressure, magnetic field, supply voltage, and so on. Secondly, it is due to inherent noises which are always present in nature, i.e., white noise, flicker noise, random-walk noise, and various other noise processes. The former can be greatly reduced by controlling the environment. But the latter is inevitable and uncontrollable in most situations. Since we are interested in setting up a clock noise model and studying clock stability, we consider only the second one. This is a reasonable assumption if the environmental effect is minimized.

B. Background of the Clock Noise Modeling

To describe the background of the clock noise modeling, we closely follow the work of Barnes et al. [1]. Consider a timing device which generates stable clock pulses. Assume that an instantaneous output voltage V(t) of the device is given by

$$V(t) = (V_0 + \varepsilon(t)) \sin (2\pi f_0 t + \phi(t)) \tag{1.1}$$

where V_0 and f_0 are the nominal amplitude and frequency, respectively. If there is no nonlinear modulation effect of converting amplitude changes to phase changes and the following conditions are satisfied

$$\left| \frac{\varepsilon(t)}{V_0} \right| < 1 \tag{1.2}$$

and

$$\left| \frac{\phi'(t)}{2\pi f_0} \right| < 1 \tag{1.3}$$

then the instantaneous phase $\Phi(t)$ is

$$\Phi(t) = 2\pi f_0 t + \phi(t) \tag{1.4}$$

Instantaneous frequency $\Phi'(t)$ is obtained from a derivative of the instantaneous phase. Thus,

$$\begin{aligned} \Phi'(t) &= 2\pi f_0 + \phi'(t) \qquad (1.5) \\ &= 2\pi f_0 \left(1 + \frac{\phi'(t)}{2\pi f_0} \right) \\ &= 2\pi f_0 \left(1 + \Omega(t) \right) \end{aligned}$$

where the instantaneous fractional frequency deviation $\Omega(t)$ from the nominal frequency f_0 is defined by

$$\Omega(t) = \frac{\phi'(t)}{2\pi f_0} \tag{1.6}$$

Since we deal with the clock noise processes, single-sided power spectral density $S_\Omega(f)$ of $\Omega(t)$ is considered. It is known that $S_\Omega(f)$ is expressed in the form of Laurent series expansion in the annular region of the frequency plane excluding the singularity at f=0 [1]. That is

$$S_\Omega(f) = \sum_{i=-\infty}^{\infty} h_i f^i , \qquad \text{for } 0 < f \leq f_h \tag{1.7}$$

where h_i is a constant dependent upon each clock device and f_h is a high frequency bandlimit. It was proposed that the power spectral density $S_\Omega(f)$ of $\Omega(t)$ can be used to define the frequency stability [1]. But in practice, it is sufficient to use only few terms for $S_\Omega(f)$ such that

$$S_\Omega(f) = h_{-2}f^{-2} + h_{-1}f^{-1} + h_0 + h_1 f + h_2 f^2 \tag{1.8}$$

In the above equation, the first term is called a random-walk frequency noise, the second is a flicker frequency noise, and the third is a white frequency noise. The fourth is a kind of flicker noise. And the last is of the random-walk noise type. In other words, if the flicker noise is generated by some method, then other power spectral densities with higher odd powers in f can be obtained by post-cascading integrators with their inputs being flicker noise which is generated by the same method, but with different input noise power. And the power spectral densities with higher even power in f may be treated in a

similar way by feeding a white noise or a random-walk noise. For this reason, we are interested in realizing only the first three components as the major clock noise processes. Thus, rewrite $S_\Omega(f)$ as follows:

$$S_\Omega(f) = h_{-2}f^{-2} + h_{-1}f^{-1} + h_0 \tag{1.9}$$

The block diagram for the clock noise model is shown in Figure 1. In the figure, $w_0(t)$, $w_{-1}(t)$, and $w_{-2}(t)$ are assumed to be mutually independent white noise with zero means and spectral amplitudes S_w, S_f, and S_r, respectively. The relation between these spectral amplitudes and h_i's can be determined as follows.

From Figure 1, $S_\Omega(f)$ is given by

$$S_\Omega(f) = 2 \left(S_w + \frac{1}{2\pi f}S_f + \frac{1}{(2\pi f)^2}S_r \right) \tag{1.10}$$

Here, multiplication factor 2 is included to match the single-sided power spectral density in equation (1.9). Comparing equation (1.10) to equation (1.9), we have

$$S_w = \frac{1}{2}h_0 \tag{1.11a}$$

$$S_f = \pi h_{-1} \tag{1.11b}$$

$$S_r = 2\pi^2 h_{-2} \tag{1.11c}$$

As shown in Figure 1, the problem is how to realize an irrational transfer function $\frac{1}{\sqrt{s}}$. The other two are trivial to realize. In Chapter II, we will examine properties of these three noise processes. And we will show, in Chapter III, that this kind of irrational transfer function can be approximated by a rational function in s with a desired

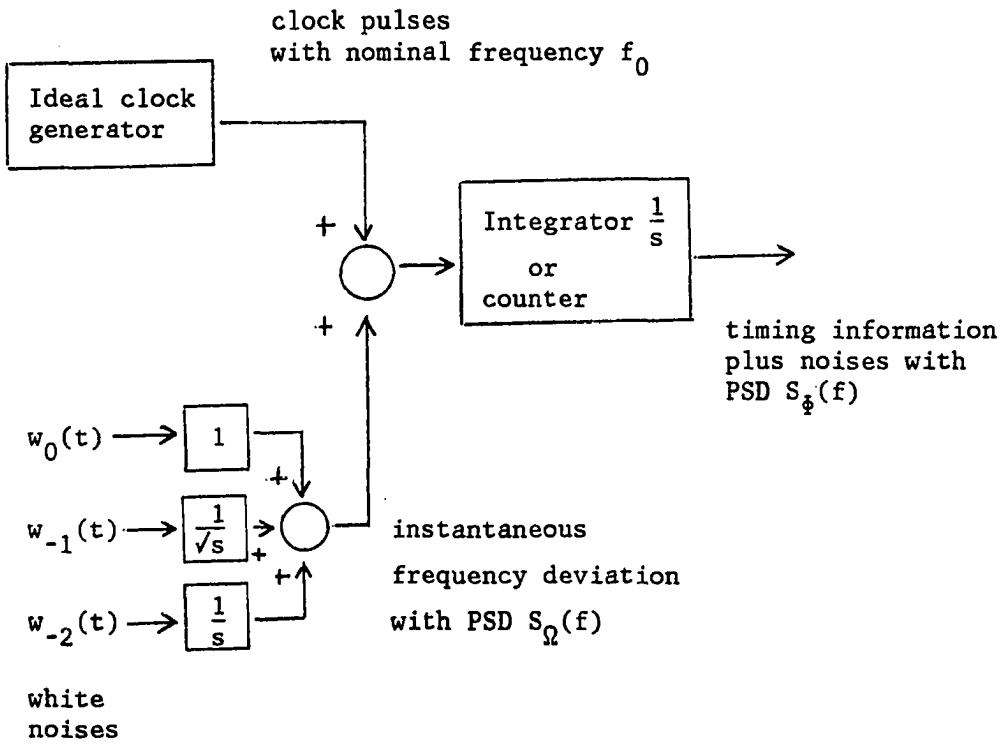

FIGURE 1. A clock noise model

degree of accuracy in a fixed frequency range. In Chapter IV, realization of state model of clock noises to the estimation and prediction of timing error will be discussed using Kalman filtering. Its application will be described in Chapter V. Chapter VI will be devoted for summary and conclusion of the work.

II. CHARACTERISTICS OF THE CLOCK NOISE PROCESSES

In this chapter, we consider the characteristics of white and random-walk noise processes briefly and study the flicker noise characteristics in detail.

A. White Noise

It is defined to have a constant spectral density function in the entire frequency range. With the spectral amplitude A, the power spectral density $S_w(j\omega)$ is given by

$$S_w(j\omega) = A \tag{2.1}$$

The corresponding autocorrelation function is then

$$R_w(\tau) = A\delta(\tau) \tag{2.2}$$

A constant spectral density function is non-integrable and so is a physical fiction [2]. All physical systems are bandlimited to some extent and thus no such an ideal spectral density function exists. To avoid a notion of infinite variance of the white noise, we assume that the system is bandlimited and so is the white noise. For more information, see Brown [3].

B. Random-walk Noise

As shown in Figure 1, the continuous version of a random-walk process can be generated as the output of an integrator driven by a white noise with unity spectral amplitude. In Figure 2, the random-walk

noise r(t) is given by

$$r(t) = \int_0^t w(u)\, du \tag{2.3}$$

Then,

$$E[r(t)] = 0 \tag{2.4}$$

$$E[r^2(t)] = t \tag{2.5}$$

Note that the variance increases linearly with time t and the root mean square value increases in proportion to $\sqrt{t}$. It is an evolutionary process. See reference [3] for detail.

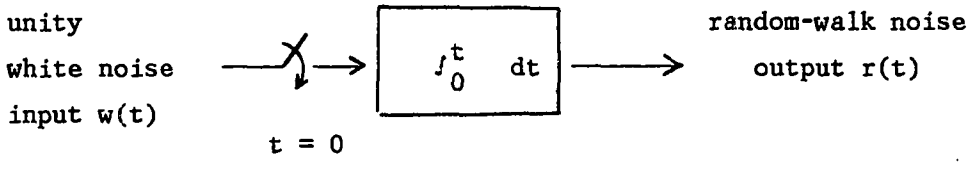

FIGURE 2. Random-walk noise generator

C. Flicker Noise

Flicker noise has been known in many scientific experiments for many decades. But its physical origin has not been fully understood yet. It is found in various areas such as in the study of semiconductor devices, in music, in the fluctuation of an atomic frequency standard, in the rotational change of the earth, and so on [4-7]. Since its spectral density function varies in accordance with $|f|^{-\alpha}$ for $\alpha \simeq 1$ over a significant range of the frequency, it is also called $\frac{1}{f}$ noise. We will mainly consider the case with a fixed $\alpha = 1$.

1. Properties of flicker noise

The power spectral density of flicker noise is given by

$$S_f(j\omega) = \frac{1}{|\omega|} \tag{2.6}$$

$S_f(j\omega)$ is unbounded at zero frequency and is not integrable up to infinite frequency. This implies that the total power is not defined over the entire frequency range $[0, \infty]$. Let's consider the power P in the frequency range $[\omega_1 , \omega_2]$.

$$P = 2 \frac{1}{2\pi} \int_{\omega_1}^{\omega_2} S_f(j\omega)\, d\omega \tag{2.7}$$

$$= \frac{1}{\pi} \int_{\omega_1}^{\omega_2} \frac{1}{|\omega|}\, d\omega$$

$$= \frac{1}{\pi} \ln\left(\frac{\omega_2}{\omega_1}\right)$$

From equation (2.7), we can draw some inherent characteristics of the flicker noise. If the frequency ratio $\frac{\omega_2}{\omega_1}$ is fixed, then the power is same in the lower or higher frequency range with same ratios. This is called the 'scale invariance principle'. Since we have an unboundedness condition in both frequency extremes, P in either of the following two cases has a special name.

If ω_1 = fixed and $\omega_2 \to \infty$, then $P \to \infty$ (ultraviolet catastrophe)

If $\omega_1 \to 0$ and ω_2 = fixed, then $P \to \infty$ (infrared catastrophe)

It was pointed out that these mentally annoying problems arise from a simple error of trying to extrapolate experimental results beyond their range of applicability and direct observation [8,9]. If we consider that every measuring device has a high frequency bandwidth limit and even a physical system itself has such a limit, the concept of the ultraviolet catastrophe never causes any trouble.

Concerning the lower frequency limit, its existence was postulated for a long time. Since in the absence of that limit the difficulty of dealing with the infrared catastrophe arises. But experimental results have not confirmed the existence of the lower limit. On the contrary, many experiments showed that it can be as close to zero as the observation permits. In one paper [10], it is reported that they observed it down to 5×10^{-7} Hz which corresponds to 2×10^{6} seconds ($\simeq$ 23.2 days). Since it is almost impossible to cary out an experiment with a very long observation time interval, the determination of the lower frequency limit in the experiment must be traded for the length of

observation. Therefore, we never get into trouble with the infrared catastrophe in an experiment which takes finite time to be finished.

Flinn gives an interesting argument to determine the extent of the flicker noise spectrum [11]. In his short paper, he assumed the lower limit of 10^{-17} Hz (≃ 3.2 billion years) corresponding to a current estimate of the age of the universe. And the upper limit may be fixed by considering the time taken for light to traverse the classical radius of the electron. It is about 10^{23} Hz. Then, the total spectrum range becomes 40 decades. Root mean square (RMS) value of this 40 decades power spectrum would be about only six times as great as the power in the range between 1 and 10 Hz. This tells us that flicker noise is a divergent process, but its divergent characteristic is weak compared to random-walk noise. In fact, flicker noise has a logarithmic divergence property, whereas random-walk noise diverges in proportion to time t as shown in equation (2.5).

2. Nonstationarity of flicker noise

In order to see that the process is nonstationary, consider the flicker noise output f(t) shown in Figure 3. The impulse response of the system, h(t), is given by

$$h(t) = L^{-1}\left(\frac{1}{\sqrt{s}}\right) \tag{2.8}$$

$$= \frac{1}{\sqrt{\pi t}}$$

Thus, f(t) is written in the convolution form of h(t) and input w(t) as follows:

$$f(t) = w(t) * h(t) \tag{2.9}$$

$$= \int_0^t w(u) \frac{1}{\sqrt{\pi(t-u)}}\, du$$

where * denotes a convolution.

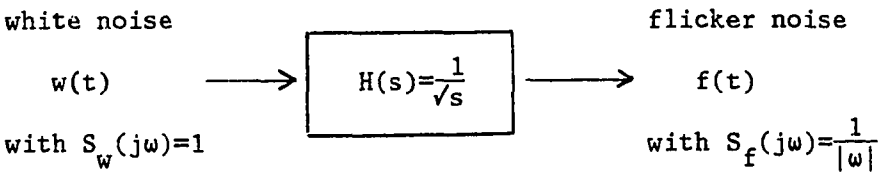

FIGURE 3. Flicker noise generated from a white noise source

Then, the autocorrelation function $R_f(t,t+\tau)$ of the flicker noise f(t) becomes

$$R_f(t,t+\tau) = E[f(t)f(t+\tau)] \tag{2.10}$$

$$= E\left[\int_0^t \int_0^{t+\tau} \frac{1}{\sqrt{\pi(t-u)}} \frac{1}{\sqrt{\pi(t+\tau-v)}} w(u)w(v)\, du\, dv \right]$$

$$= \frac{1}{\pi} \int_0^t \frac{1}{\sqrt{(t-u)(t+\tau-u)}}\, du$$

$$= \frac{1}{\pi} \ln\left[2 \{\sqrt{t^2+\tau t}+t+\frac{\tau}{2}\}/\tau \right]$$

Here, we used the property $E[w(u)w(v)] = \delta(u-v)$ for the white noise.

From equation (2.10), we find out that the variance (mean square value) is not defined, when $\tau = 0$. This is expected because the impulse response h(t) is unbounded at the time when the input is applied.

When $t >> \tau > 0$,

$$R_f(t,t+\tau) = \frac{1}{\pi} \ln(\frac{4t}{\tau}) \tag{2.11}$$

This shows a logarithmic increase of the autocorrelation function as time increases and thus flicker noise is a nonstationary process.

Since it is a nonstationary process, we may not use many well-developed methods for stationary processes. We may even consider using a less familiar evolutionary process approach which is usually not successful for getting any meaningful results [1,8,9].

But as pointed out earlier, it is not unreasonable to restrict frequency to a range of interest. Consider a bandlimited flicker noise with the power spectral density as follows:

$$S_f(j\omega) = \begin{cases} \frac{1}{|\omega|} & \text{for } \omega_1 \le \omega \le \omega_2 \\ 0 & \text{otherwise} \end{cases} \tag{2.12}$$

Then, it has finite power in the defined frequency range and becomes a stationary process. We will next compute the autocorrelation function of the process using equation (2.12).

$$R_f(\tau) = \frac{1}{2\pi} \int_{-\infty}^{\infty} S_f(j\omega)\, e^{j\omega\tau}\, d\omega \qquad (2.13)$$

$$= \frac{1}{2\pi}\, 2 \int_{\omega_1}^{\omega_2} \frac{1}{|\omega|}\, e^{j\omega\tau}\, d\omega$$

$$= \frac{1}{\pi} \left[C_i(\omega_2\tau) - C_i(\omega_1\tau) \right]$$

where $C_i(z)$ is the cosine integral which has a following power series representation [12].

$$C_i(z) = \gamma + \ln z + \sum_{k=1}^{\infty} \frac{(-1)^k z^{2k}}{(2k)!\ 2k}\ , \quad |\arg z| < \pi \qquad (2.14)$$

where γ is an Euler constant.

Substituting $C_i(z)$ into $R_f(\tau)$, we have

$$R_f(\tau) = \frac{1}{\pi} \left[\ln\left(\frac{\omega_2}{\omega_1}\right) + \sum_{k=1}^{\infty} \frac{(-1)^k}{(2k)!\ 2k} \left\{ (\omega_2\tau)^{2k} - (\omega_1\tau)^{2k} \right\} \right] \qquad (2.15)$$

Now the mean square power is defined when $\tau = 0$. Note that $R_f(\tau)$ is only a function of τ as compared to equation (2.10) which is a function of both t and τ.

3. Considerations on the generation of the flicker noise

Many methods have been proposed to model a flicker noise process and generate a process having flicker noise-like characteristics. Redeka [13] reviews some of the methods. Here, we present some of them for a brief discussion.

a. Distributed RC - line model In the RC transmission line based on the diffusion equation, line impedance Z is typically written by $\sqrt{(\frac{r}{j\omega c})}$, where r and c are resistance and capacitance per unit length of the transmission line, respectively. If a noise current input is injected into the line, the spectral density of the output noise voltage follows the flicker noise characteristic.

b. Halford's mechanical model (superposition of relaxation process) Halford considered a set of some random perturbations subject to certain constraints [14]. The set is characterized by $P(\tau)$ and $A^2(\tau)$, where $P(\tau)$ is the probability density of perturbations with time constant τ and $A^2(\tau)$ is a mean square amplitude of perturbations having a time constant τ. For a case concerning flicker noise, the following constraint must be satisfied

$$P(\tau)A^2(\tau) \propto B \frac{1}{\tau^2} \tag{2.16}$$

One choice for this is that all constants are equally probable, i.e., $P(\tau) = 1$, and $A(\tau) = \frac{1}{\tau} e^{-(t/\tau)}$, $t \geq 0$. Hence, the spectral density of the set of perturbations $A(\tau)$ for the time constant τ is $\frac{1}{1+\omega^2\tau^2}$. Then, the spectral density of the set over the range of τ from 0 to ∞ has a flicker noise characteristics.

$$\int_0^\infty \frac{1}{1+\omega^2\tau^2}\, d\tau = \left[\frac{1}{|\omega|} \tan^{-1}(\omega\tau) \right]_0^\infty \qquad (2.17)$$

$$= \frac{\pi}{2} \frac{1}{|\omega|}$$

c. Half-order integrator If white noise with a power spectral density $S_w(j\omega) = A$ is integrated m times with respect to time successively, then the PSD of the resulting process f(t) becomes

$$S_f^{(m)}(j\omega) = \frac{A}{|\omega|^{2m}} \qquad (2.18)$$

If $2m = 1$ is chosen, then

$$S_f^{(\frac{1}{2})}(j\omega) = \frac{A}{|\omega|} \qquad (2.19)$$

which is the PSD of the flicker noise. The condition $m = \frac{1}{2}$ requires a notion of the hypothetical half-order integrator [9,15-17]. And this leads to a special case of a general mathematical concept of fractional order integration.

d. Lumped-parameter approximation of impulse response If the problem can be solved by constructing a linear filter having a transfer function, $H(s) = \frac{1}{\sqrt{s}}$, it leads to a realization by using distributed or lumped parameter networks.

Our approach of the continued fraction expansion method to be described in the next chapter is based upon this method, in other words, the shaping filter method.

Considering the impulse response of the shaping filter with t_0 being the instant when the input is applied, we get from equation (2.8) $h(t,t_0) = \frac{1}{\sqrt{\pi(t-t_0)}}$. Notice that $h(t,t_0)$ is not decomposable into a product of arbitrary functions of $M(t)$ and $N(t_0)$ such that $h(t,t_0) = M(t)N(t_0)$. It is well known that a system is realizable by a finite dimensional linear system, if and only if the system is factorable as above [18].

For this reason, the system we consider cannot be realized by a linear system with finite dimension. The dimension of the system must be infinite. Thus, our approach is not a perfect solution but is an approximation and a compromise between the simplicity rendered by the finite dimensional system and the accuracy of the infinite dimensional system.

In the next chapter, the finite dimensional linear system having a rational transfer function approximation is considered. We will review some techniques and discuss our method for doing this.

III. APPROXIMATION OF THE FLICKER NOISE

A. Modeling of the Flicker Noise Process with Finite-Order System

We are familiar with a rational transfer function description in the frequency domain which represents an output of a system driven by an input. Most linear system theories extensively deal with such a finite order transfer function of a lumped linear time-invariant system without having any nonlinearity, delay, or time-varying components. Since the transfer function approach is easy to apply and gives a reasonably good result to engineering problems, it has been widely used. Furthermore, it is readily converted into a state-space description and then its realization is straightforward by using known canonical forms.

But in most cases, a process itself cannot be expressed in the form of a rational function. The rational transfer function is regarded as a linearization of a complicated system response in general. Flicker noise has an irrational transfer function as discussed in earlier sections. Its transfer function $\frac{1}{\sqrt{s}}$ is shown in Figure 1. In the next section, we examine several methods to obtain a rational approximation for this kind of the transfer function.

1. Staircase approximation

The basic idea for realizing $H(s) = \frac{1}{\sqrt{s}}$ can be described as how to assign poles and zeros in the complex frequency plane according to a rule, whatever it may be. The simplest one is just to alternate simple

poles and zeros on the negative real axis in the frequency plane. This is illustrated with the Bode plot shown in Figure 4. By doing so, stability and minimal phase are always guaranteed.

To illustrate this further, let $H_A(s)$ be a transfer function of an approximation with poles at $s = -a_i$, $i = 1, 2, \ldots, N$ and zeros at $s = -b_i$, $i = 1, 2, \ldots, N$, and $a_i < b_i$. Then

$$H_A(s) = K \frac{(s+b_1)(s+b_2)(s+b_3) \ldots (s+b_N)}{(s+a_1)(s+a_2)(s+a_3) \ldots (s+a_N)} \tag{3.1}$$

where K is a gain factor.

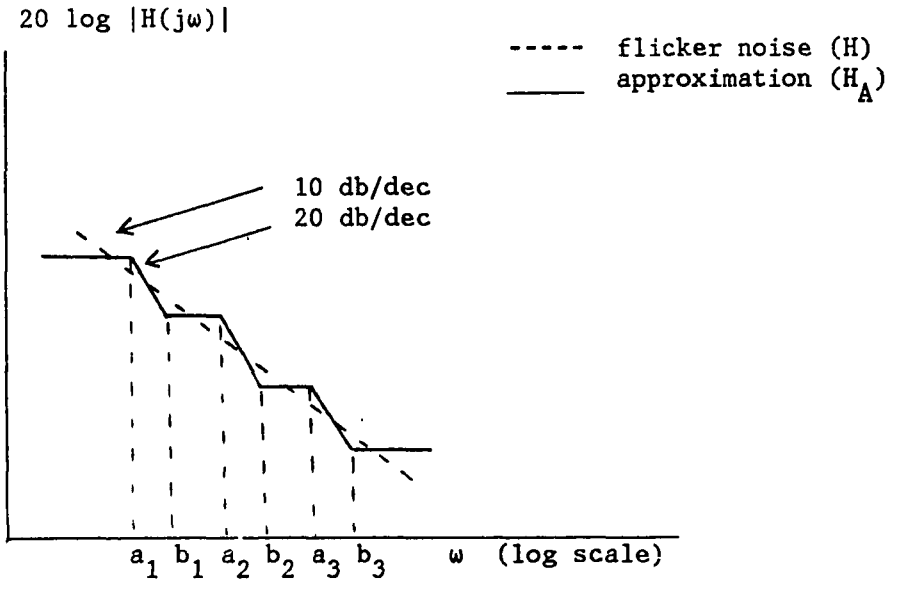

FIGURE 4. Staircase approximation

It is known that $H_A(s)$ in equation (3.1) is a driving-point impedance of an RC one-port. In order to get an exact matching, an infinite number of poles and zeros are required. It is practically impossible to specify an innumerable number of parameters. What we are interested in is to determine the parameters to give a good match over a finite frequency range.

To determine K, a_i's, and b_i's properly, consider a minimization of an error functional in the least square sense. Since the frequency response at a discrete set of frequencies, $\{\omega_j, j = 1, 2, \ldots, M\}$ is known, an error functional E can be defined with a weighting factor d_j at each frequency ω_j.

$$E = \sum_{j=1}^{M} d_j \left| \frac{1}{\sqrt{\omega_j}} - K \prod_{i=1}^{N} \{(\omega_j^2 + b_i^2)/(\omega_j^2 + a_i^2)\}^{1/2} \right|^2 \qquad (3.2)$$

Minimizing E with respect to each parameter, we get

$$\frac{\partial E}{\partial K} = 0 \qquad (3.3)$$

$$\frac{\partial E}{\partial a_i} = 0 \quad , \qquad i = 1, 2, \ldots, N \qquad (3.4)$$

$$\frac{\partial E}{\partial b_i} = 0 \quad , \qquad i = 1, 2, \ldots, N \qquad (3.5)$$

The parameters are determined by solving (2N + 1) nonlinear algebraic equations. The main disadvantage of this least square minimization is that the complexity builds up fast as pairs of poles and zeros are added to expand the frequency range.

2. Approximation of spectral density function by a class of orthogonal functions

The spectral density of the flicker noise $S_f(j\omega) = \frac{1}{|\omega|}$ is considered instead of directly manipulating $|H(j\omega)| = \frac{1}{\sqrt{\omega}}$. Let $R_f(\tau)$ be an autocorrelation function corresponding to $S_f(j\omega)$. Then, the key idea is how to approximate the spectral density of a random process by a set of rational functions of ω^2, provided that $R_f(\tau)$ is expressed by a linear combination of orthonormal functions $\{\psi_n(\tau)\}$ derived from an exponential function set $\{ e^{-c\tau}, c^{-2c\tau}, c^{-3c\tau}, \ldots \}$, c = constant. These exponential functions are neither normal nor orthogonal. But by the Gram-Schmidt orthogonalization method, a linear combination of these functions is systematically formed. See reference [19] for detail. Then, $R_f(\tau)$ can be written by

$$R_f(\tau) = \sum_{n=1}^{N} B_n \psi_n(\tau) \ , \ B_n = \text{const} \tag{3.6}$$

Since the orthogonal functions $\psi_n(\tau)$ are derived from a set of exponential functions, they can be rewritten as functions of $e^{-nc|\tau|}$, $n = 1, 2, \ldots, N$.

$$R_f(\tau) = \sum_{n=1}^{N} A_n e^{-nc|\tau|} \ , \ A_n = \text{const} \tag{3.7}$$

Then, the weighting function (impulse response) of the system can be fixed in the same form of equation (3.7). That is

$$h(t) = \sum_{n=1}^{N} A_n' \, e^{-nct} \ , \ t \geq 0 \tag{3.8}$$

where A_n' can be determined from A_n. Then, the corresponding transfer function becomes

$$H(s) = \sum_{n=1}^{N} \frac{A_n'}{s+nc} \tag{3.9}$$

which is a proper rational transfer function in s. Thus, the main key is to find a proper 'c', but it is difficult to determine 'c' for a considerably wide frequency range.

3. Steiglitz's method

Steiglitz's method [20] is based on a simple observation that

$$\lim_{n\to\infty} \left(1 - \frac{1}{\sqrt{s}} \right)^n \to 0 \qquad \text{if} \quad \left| 1 - \frac{1}{\sqrt{s}} \right| < 1 \tag{3.10}$$

Equation (3.10) is expanded as a binomial series and the odd and even power terms in $\frac{1}{\sqrt{s}}$ are collected separately. Let n be odd. Define $Z_n(s)$ with $n \to \infty$ as follows:

$$Z_n(s) = \frac{\sum_{k=0,2,\ldots}^{n-1} \binom{n}{k} s^{-k/2}}{\sum_{k=1,3,\ldots}^{n} \binom{n}{k} s^{-(k-1)/2}} \to \frac{1}{\sqrt{s}}$$

$$= \frac{(1+\sqrt{s})^n - (1-\sqrt{s})^n}{(1+\sqrt{s})^n + (1-\sqrt{s})^n} \cdot \frac{1}{\sqrt{s}} \tag{3.11}$$

Then, poles and zeros of $Z_n(s)$ are located on the negative real axis at the following points:

$$\text{zeros} : \quad Z_k = -\tan^2\left(\frac{k\pi}{n}\right) \quad , \quad k = 1, 2, \ldots , (n-1)/2 \tag{3.12}$$

$$\text{poles} : \quad P_k = -\{\tan^2\left(\frac{k\pi}{n}\right)\}^{-1} \quad , \quad k = 1, 2, \ldots , (n-1)/2 \tag{3.13}$$

Then, the partial fraction expansion of $Z_n(s)$ becomes

$$Z_n(s) = \frac{1}{n} + \frac{2}{n} \sum_{k=1}^{(n-1)/2} \frac{1 - P_k}{s - P_k} \tag{3.14}$$

Since all poles lie on the negative real axis and have positive residues, $Z_n(s)$ is an RC driving-point impedance. Unit step response of $Z_n(s)$ shows a good matching for $t < \frac{1}{4}\pi n^2$.

B. Continued Fraction Expansion of $s^{-\frac{1}{2}}$

We adopt a continued fraction expansion method to get a rational approximation. By using this method, we show that an approximant to the irrational function $\frac{1}{\sqrt{s}}$ can be generated iteratively. It can be considered a generalization of Steiglitz's method discussed in the previous section. Let $P_n(s)$ and $Q_n(s)$ be two sequences of polynomials in s which are coprime with each other. Let a and K be arbitrary constants. The polynomials $P_n(s)$ and $Q_n(s)$ will be defined as follows (with $P_0 = 1$ and $Q_0 = 1$):

$$P_n(s) = aP_{n-1}(s) + K^2Q_{n-1}(s) \quad , \qquad n = 0, 1, 2, \ldots \tag{3.15}$$

$$Q_n(s) = sP_{n-1}(s) + aQ_{n-1}(s) \quad , \qquad n = 0, 1, 2, \ldots \tag{3.16}$$

And form a rational transfer function $R_n(s)$.

$$R_n(s) = \frac{P_n(s)}{Q_n(s)} \quad , \quad n = 0, 1, 2, \ldots \tag{3.17}$$

Then, $\{R_n(s)\}_{n=1}^{n=\infty}$ is a sequence of rational functions in s. If $R_n(s)$ is assumed to converge to a rational function R(s), as $n \to \infty$ (this will be shown later), we get

$$R_n(s) = \frac{P_n(s)}{Q_n(s)} \quad , \quad n = 0, 1, 2, \ldots \tag{3.18}$$

$$= \frac{aP_{n-1} + K^2Q_{n-1}}{sP_{n-1} + aQ_{n-1}}$$

$$= \frac{aR_{n-1} + K^2}{sR_{n-1} + a}$$

Since it is assumed that $R_n(s) \to R(s)$, $R_{n-1}(s) \to R(s)$ as $n \to \infty$, it becomes

$$R(s) = \frac{aR(s) + K^2}{sR(s) + a}$$

or

$$sR^2(s) + aR(s) = aR(s) + K^2$$

Solving for R(s), we get

$$R(s) = \pm \frac{K}{\sqrt{s}} \tag{3.19}$$

When K = 1, we obtain the desired transfer function. This kind of a technique has been used in many references [21-24].

To obtain a recursive formula for $R_n(s)$, adopt a matrix notation. From equations (3.15) and (3.16), we get

$$\begin{bmatrix} P_n(s) \\ Q_n(s) \end{bmatrix} = \begin{bmatrix} a & K^2 \\ s & a \end{bmatrix} \begin{bmatrix} P_{n-1}(s) \\ Q_{n-1}(s) \end{bmatrix} \tag{3.20}$$

$$= \begin{bmatrix} a & K^2 \\ s & a \end{bmatrix}^2 \begin{bmatrix} P_{n-2}(s) \\ Q_{n-2}(s) \end{bmatrix}$$

.

.

$$= \begin{bmatrix} a & K^2 \\ s & a \end{bmatrix}^n \begin{bmatrix} 1 \\ 1 \end{bmatrix}$$

Then, the sequence $\{R_n(s)\}_{n=1}^{n=\infty}$ is obtained as follows:

$$R_1(s) = \frac{a+K^2}{s+a} \tag{3.21}$$

$$R_2(s) = \frac{K^2s+2K^2a+a^2}{(2a+K^2)s+a^2} \tag{3.22}$$

$$R_3(s) = \frac{(3aK^2+K^4)s+3K^2a^2+a^3}{K^2s^2+(3aK^2+3a^3)s+a^3} \tag{3.23}$$

.

.

.

The parameter 'a' can be varied to get different approximations for different frequency ranges. K can be used for either gain or frequency response adjustment.

From equation (3.20), define a matrix U as follows:

$$U = \begin{bmatrix} a & K^2 \\ s & a \end{bmatrix} \tag{3.24}$$

Then, the problem is reduced to finding an expression for U^n in s. Since eigenvalues of the matrix U are $\lambda_1 = a + K\sqrt{s}$, $\lambda_2 = a - K\sqrt{s}$, by using the Cayley-Hamilton theorem [18], set as follows:

$$U^n = C_n I + D_n U \tag{3.25}$$

$$= C_n \begin{bmatrix} 1 & 0 \\ 0 & 1 \end{bmatrix} + D_n \begin{bmatrix} a & K^2 \\ s & a \end{bmatrix}$$

$$= \begin{bmatrix} C_n + aD_n & K^2 D_n \\ sD_n & C_n + aD_n \end{bmatrix}$$

where C_n and D_n are constants to be determined, and I is an identity matrix.

C_n and D_n are determined by solving the following two equations simultaneously.

$$\lambda_1^n = C_n + D_n \lambda_1 \tag{3.26}$$

$$\lambda_2^n = C_n + D_n \lambda_2 \tag{3.27}$$

Thus,

$$C_n = \frac{1}{\lambda_1 - \lambda_2} \left(\lambda_1\lambda_2^n - \lambda_1^n\lambda_2\right) \tag{3.28}$$

$$= \frac{(a+K\sqrt{s})(a-K\sqrt{s})^n - (a-K\sqrt{s})(a+K\sqrt{s})^n}{2K\sqrt{s}}$$

$$D_n = \frac{1}{\lambda_1 - \lambda_2} \left(\lambda_1^n - \lambda_2^n\right) \tag{3.29}$$

$$= \frac{(a+K\sqrt{s})^n - (a-K\sqrt{s})^n}{2K\sqrt{s}}$$

From equations (3.28), (3.29), and (3.25) we have

$$R_n(s) = \frac{K}{\sqrt{s}} \frac{\sqrt{s}\left[(a+K\sqrt{s})^n + (a-K\sqrt{s})^n\right] + K\left[(a+K\sqrt{s})^n - (a-K\sqrt{s})^n\right]}{\sqrt{s}\,\sqrt{s}\left[(a+K\sqrt{s})^n - (a-K\sqrt{s})^n\right] + K\left[(a+K\sqrt{s})^n + (a-K\sqrt{s})^n\right]} \tag{3.30}$$

$$= \frac{K}{\sqrt{s}} \frac{(a+K\sqrt{s})^n(K+\sqrt{s}) - (a-K\sqrt{s})^n(K-\sqrt{s})}{(a+K\sqrt{s})^n(K+\sqrt{s}) + (a-K\sqrt{s})^n(K-\sqrt{s})} \tag{3.31}$$

Many different rational approximations are possible from equation (3.31). For instance, let $K^2 = a$. Then, we have

$$R_n(s) = \sqrt{\left(\frac{a}{s}\right)} \frac{\{1+\sqrt{\left(\frac{s}{a}\right)}\}^{n+1} - \{1-\sqrt{\left(\frac{s}{a}\right)}\}^{n+1}}{\{1+\sqrt{\left(\frac{s}{a}\right)}\}^{n+1} + \{1-\sqrt{\left(\frac{s}{a}\right)}\}^{n+1}}$$

Using the binomial expansion, we have

$$R_n(s) = \frac{\sum_{k=0}^{[n/2]} \binom{n+1}{2k+1} \left(\frac{s}{a}\right)^k}{\sum_{k=0}^{[(n+1)/2]} \binom{n+1}{2k} \left(\frac{s}{a}\right)^k} \qquad (3.32)$$

where [p] means the greatest integer $\leq p$, and then the highest order of the denominator polynomial is $[\frac{(n+1)}{2}]$.

Another form of approximation can be derived from equation (3.30) by setting K = 1. That is

$$R_n(s) = \frac{1}{\sqrt{s}} \frac{\sqrt{s}[(a+\sqrt{s})^n + (a-\sqrt{s})^n] + [(a+\sqrt{s})^n - (a-\sqrt{s})^n]}{\sqrt{s}[(a+\sqrt{s})^n - (a-\sqrt{s})^n] + [(a+\sqrt{s})^n + (a-\sqrt{s})^n]} \qquad (3.33)$$

$$= \frac{\sum_{k=0}^{[n/2]} [\binom{n}{2k} a^{-2k} + \binom{n}{2k+1} a^{-2k-1}] s^k}{\sum_{k=0}^{[n/2]} [\binom{n}{2k-1} a^{-2k+1} + \binom{n}{2k} a^{-2k}] s^k}$$

where $\binom{n}{r} = 0$ if $r > n$ or $r < 0$.

In both equations (3.32) and (3.33), 'a' can be varied so that the adjustment for different frequency ranges is easily made. A special case with a = 1 in equations (3.32) and (3.33) is given as follows:

$$R_n(s) = \frac{1}{\sqrt{s}} \frac{(1+\sqrt{s})^{n+1} - (1-\sqrt{s})^{n+1}}{(1+\sqrt{s})^{n+1} + (1-\sqrt{s})^{n+1}} \tag{3.34}$$

$$= \frac{\sum_{k=0}^{[n/2]} \binom{n+1}{2k+1} s^k}{\sum_{k=0}^{[(n+1)/2]} \binom{n+1}{2k} s^k} \tag{3.35}$$

Figures 5 and 6 show the frequency and unit step time responses of $R_n(s)$, corresponding to equation (3.35), for various values of n along with the ideal response of $\frac{1}{\sqrt{s}}$ for comparison.

1. Uniform convergence

It can be shown that equation (3.34) is uniformly convergent in the annular region of $D = \{s : \delta^2 \leq |s| \leq 1, 0 < \delta < 1\}$. The reason why we consider this region D in the s-domain is that it corresponds to time $t \in [1, \infty)$ in the time domain. Since flicker noise is a slowly divergent process, we are interested in long time behavior for $t \geq 1$. Consider the following for $0 < |s| < 1$.

$$\left| \frac{1}{\sqrt{s}} - R_n(s) \right| = \left| \frac{1}{\sqrt{s}} - \frac{(1+\sqrt{s})^{n+1} - (1-\sqrt{s})^{n+1}}{\sqrt{s}\{(1+\sqrt{s})^{n+1} + (1-\sqrt{s})^{n+1}\}} \right| \tag{3.36}$$

$$= \left| \frac{1}{\sqrt{s}} \frac{2(1-\sqrt{s})^{n+1}}{(1+\sqrt{s})^{n+1} + (1-\sqrt{s})^{n+1}} \right|$$

$$= \left| \frac{1}{\sqrt{s}} \frac{2}{1 + \{(1+\sqrt{s})/(1-\sqrt{s})\}^{n+1}} \right|$$

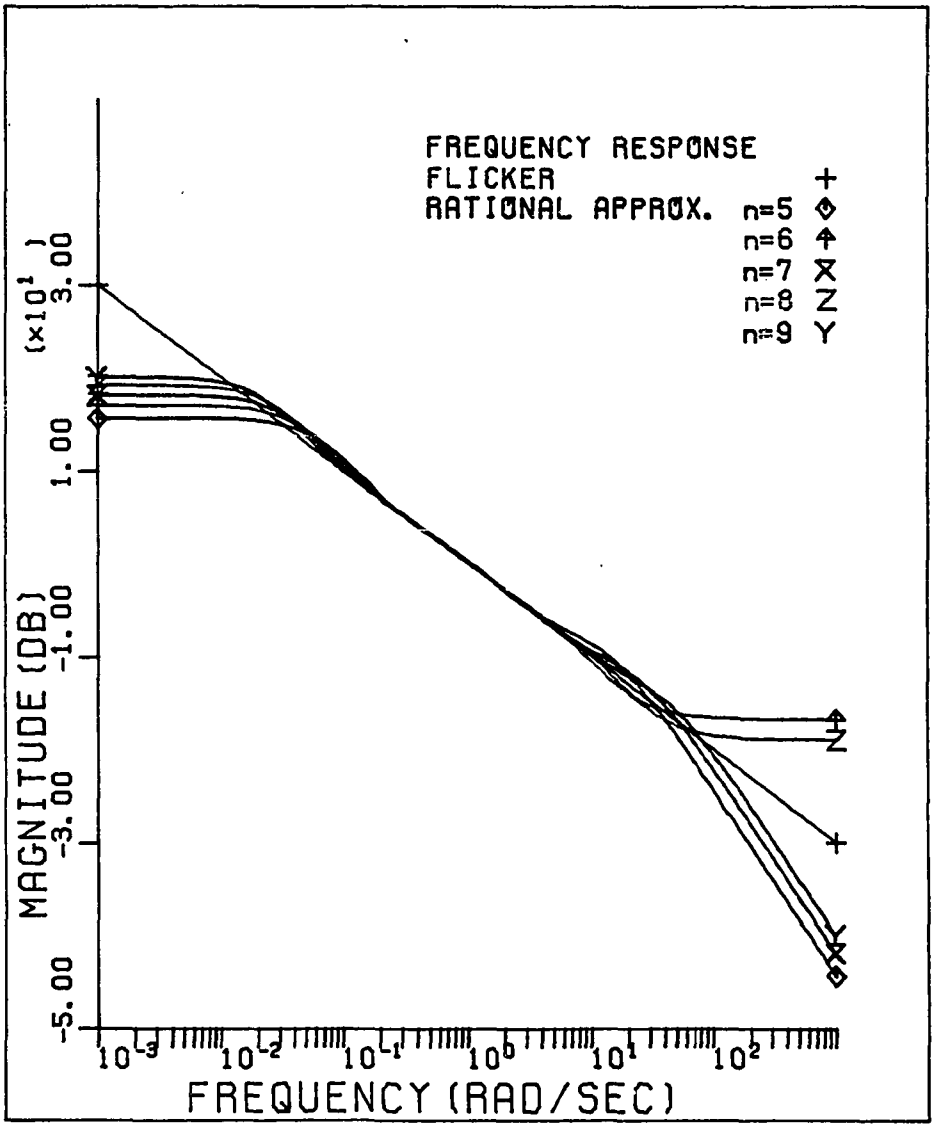

FIGURE 5. Frequency response of $R_n(s)$

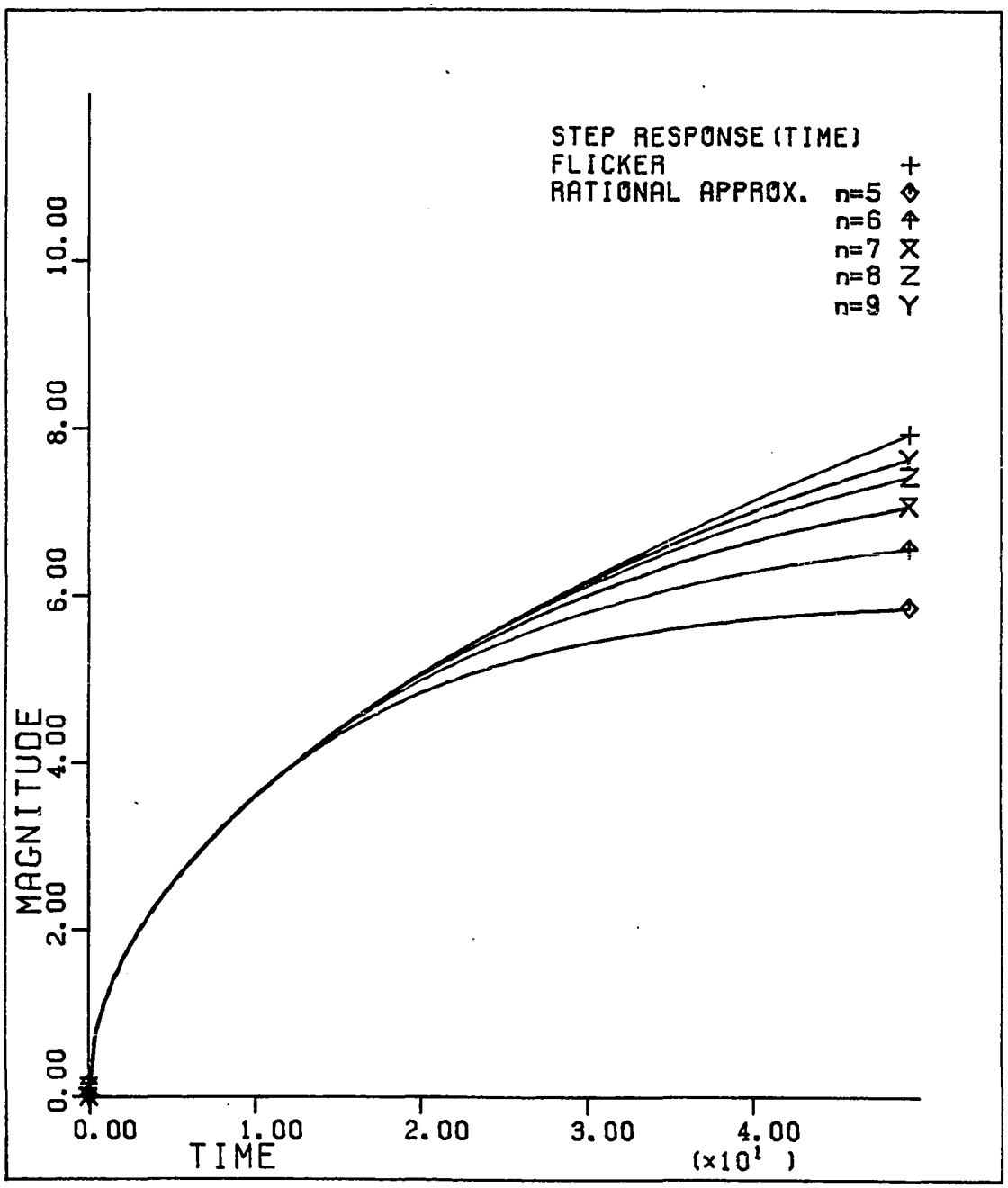

FIGURE 6. Unit step time response of $R_n(s)$

Since $|s| < 1$, it can be expanded by a geometric series. Thus, we have

$$= \left| \frac{1}{\sqrt{s}} \frac{2}{1 + \{(1+\sqrt{s})(1+\sqrt{s}+(\sqrt{s})^2+ \dots)\}^{n+1}} \right|$$

$$= \left| \frac{1}{\sqrt{s}} \frac{2}{1 + \{1+2\sqrt{s}+2s+2(\sqrt{s})^3+ \dots \}^{n+1}} \right|$$

$$\leq \frac{1}{\delta} \frac{2}{1 + (1+2\delta+2\delta^2+ \dots)^{n+1}}$$

$$< \frac{1}{\delta} \frac{2}{1 + (2\delta+2\delta^2+ \dots)^{n+1}}$$

$$= \frac{1}{\delta} \frac{2}{1 + 2^{n+1}(\delta/(1-\delta))}$$

Thus, equation (3.36) goes to zero, as n increases. When $s = 1$, it is exactly zero. Hence, $R_n(s)$ converges to $\frac{1}{\sqrt{s}}$ uniformly in D. As n gets large, $R_n(s)$ gives a more accurate approximation over a wider frequency range.

2. Poles and zeros

Let's look into some properties of $R_n(s)$ in equation (3.35) with a = 1. Refer to Table 1. First, it can be regarded as a generalization of the Steiglitz's method [20] discussed in the previous section. Secondly, coefficients of the numerator and denominator in every $R_n(s)$ alternately show coefficient patterns of the binomial expansion $(1+s)^{n+1}$, $n \geq 1$. Thirdly, all poles and zeros are simple and interlaced on the negative real axis in the s-plane.

The poles and zeros of $R_n(s)$ are located in accordance with the following equations, and a partial tabulation is given in Table 2.

$$\text{poles:} \quad P_k = -\tan^2 \frac{2k+1}{2(n+1)} \pi \quad , k = 0, 1, \ldots , [\frac{n-1}{2}] \tag{3.37}$$

$$\text{zeros:} \quad Z_k = -\tan^2 \frac{k\pi}{n+1} \quad , k = 1, 2, \ldots , [\frac{n}{2}] \tag{3.38}$$

Since poles and zeros have negative real values, the numerator and denominator of $R_n(s)$ are Hurwitz polynomials. Hence, $R_n(s)$ is stable and has a minimum phase.

From Table 2, the poles and zeros of $R_n(s)$ with even n are inversely related each other. When n is odd, the poles themselves are self-inversely related and so are the zeros. All poles and zeros of $R_n(s)$ are the zeros of $R_{2n+1}(s)$. This can be easily verified from equations (3.37) and (3.38). In fact since $R_n(s)$ can be accurate in the frequency response for the flicker noise process over the range determined by minimum and maximum of the poles in magnitude, these two provide meaningful lower and upper frequency limits of the flicker noise model. For instance, $R_5(s)$ is accurate over the range from $\omega \simeq 0.07$ to 13.9 rad/sec.

If we check a ratio of maximum pole to minimum pole in magnitude, we find out that $R_n(s)$ with odd n covers a wider frequency range than $R_{n+1}(s)$ whose n+1 is an even number. Thus, it may be safe to choose an odd n. If n is odd, then the order of denominator is greater by one than that of numerator of $R_n(s)$. Also, when $R_n(s)$ is converted into a state-space representation, it simplifies the system dynamics. Because

TABLE 1. $R_n(s)$ (See equation (3.32) with $a = 1$.)

n	$R_n(s)$
0	$\frac{1}{1}$
1	$\frac{2}{s+1}$
2	$\frac{s+3}{3s+1}$
3	$\frac{4s+4}{s^2+6s+1}$
4	$\frac{s^2+10s+5}{5s^2+10s+1}$
5	$\frac{6s^2+20s+6}{s^3+15s^2+15s+1}$
6	$\frac{s^3+21s^2+35s+7}{7s^3+35s^2+21s+1}$
7	$\frac{8s^3+56s^2+56s+8}{s^4+28s^3+70s^2+28s+1}$
8	$\frac{s^4+36s^3+126s^2+84s+9}{9s^4+84s^3+126s^2+36s+1}$
9	$\frac{10s^4+120s^3+252s^2+120s+10}{s^5+45s^4+210s^3+210s^2+45s+1}$

it is a strictly proper transfer function, there is no direct path from the input to the output of the system. And the infinite variance problem of the output is avoided, as it will be mentioned in the next chapter.

C. Relationship of the Continued Fraction Expansion to Pade Table and System Theory

It has been known that continued fraction expansion can be obtained from Pade approximants as a special case [21-25]. The Pade approximation is such as to generate a rational fraction approximation to the value of a function. In fact, the continued fraction expansion is identical to diagonal and superdiagonal elements in the Pade table. Refer to Table 3. In short, the Pade approximation is to match a formal series expansion as far as possible.

If a function f(s) has a formal power series expansion

$$f(s) \simeq f_0(s) \tag{3.39}$$
$$= \sum_{k=0}^{\infty} C_k s^k$$

Then, [m,n] one-point Pade approximant $R_{m,n}(s)$ to f(s) is of the form

$$R_{m,n}(s) = \frac{P_m(s)}{Q_n(s)} \tag{3.40}$$
$$= \frac{p_0+p_1s+p_2s^2+ \ldots +p_ms^m}{q_0+q_1s+q_2s^2+ \ldots +q_ns^n}$$

TABLE 2. Poles and zeros of $R_n(s)$ (See Table 1.)

n	pole	zero	ratio (= |max pole|/|min pole|)
1	- 1.0		
2	- 0.33333	- 3.0	
3	- 0.17157	- 1.0	33.97
	- 5.82842		
4	- 0.10557	- 9.47213	17.94
	- 1.89443	- 0.52786	
5	- 0.07180	- 3.0	193.99
	- 1.0	- 0.33333	
	-13.92817		
6	- 0.05210	-19.19562	82.77
	- 0.63596	- 1.57241	
	- 4.31194	- 0.23191	
7	- 0.03957	- 5.82842	638.78
	- 0.44646	- 1.0	
	- 2.23983	- 0.17157	
	-25.27407		
8	- 0.03109	-32.16334	242.79
	- 0.33333	- 3.0	
	- 1.42028	- 0.70409	
	- 7.54862	- 0.13247	
9	- 0.02509	- 9.47213	1589.09
	- 0.25962	- 1.89443	
	- 1.0	- 0.52786	
	- 3.85184	- 0.10557	
	-39.86327		
10	- 0.02067	-48.37397	561.08
	- 0.20856	- 4.79475	
	- 0.75083	- 1.33186	
	- 2.42123	- 0.41301	
	-11.59869	- 0.08622	

The coefficients (p_i and q_i) of polynomials $P_m(s)$ and $Q_n(s)$ are determined by

$$f_0(s) - R_{m,n}(s) = O(s^{m+n+1}) \tag{3.41}$$

where O is a 'big o'.

From equations (3.39), (3.40), and (3.41) we have

$$(C_0+C_1s+C_2s^2+ \dots)(q_0+q_1s+ \dots +q_ns^n) - (p_0+p_1s+ \dots +p_ms^m) = O(s^{m+n+1}) \tag{3.42}$$

Equating the coefficients of like powers of s leads to a set of linear algebraic equations. Normalize by setting $Q_n(0) = q_0 = 1$. Then,

$$\begin{aligned} p_0 &= C_0q_0 \\ p_1 &= C_1q_0+C_0q_1 \\ p_2 &= C_2q_0+C_1q_1+C_0q_2 \\ &\cdot \\ &\cdot \\ p_m &= C_mq_0+C_{m-1}q_1+ \dots +C_0q_m \\ 0 &= C_{m+1}q_0+C_mq_1+ \dots +C_{m-n+1}q_n \\ &\cdot \\ &\cdot \\ 0 &= C_{m+n}q_0+C_{m+n-1}q_1+ \dots +C_mq_n \end{aligned} \tag{3.43}$$

where $C_m = 0$ if $m < 0$ and $q_j = 0$ if $j > n$.

The solution to equation (3.43) is uniquely determined, provided that a Hankel matrix of the system is non-singular [26]. Concerning algorithms for the calculation of the Pade approximants, refer to references cited above.

TABLE 3. Pade approximants $R_{m,n}(s)$ and continued fraction expansion $R_n(s)$

m\n	0	1	2	3
0	$R_0(s)$	$R_1(s)$		
1		$R_2(s)$	$R_3(s)$	
2			$R_4(s)$	$R_5(s)$
3				$R_6(s)$

It is shown that, for accurate approximation over a finite range, it is best to choose m and n orders of numerator and denominator, respectively, to be equal or nearly equal [24]. In linear system theory, a transfer function $f_0(s)$ is realizable by a finite-dimensional linear system, if and only if it is a proper rational function [18]. Thus, a typical choice of m and n to satisfy the realizability condition is that the order of denominator is greater than that of numerator,

i.e., n-m > 0. We mainly consider a case n-m = 1 among rational approximants. This corresponds to the superdiagonal elements in the Pade table (see Table 3).

If f(s) has a Stieltjes series representation [23,24], then it possesses interesting properties related to the system theory. The Stieltjes series representation for $f(s) = \frac{1}{\sqrt{s}}$ at s = 1 is given by

$$f(s) = \frac{1}{\sqrt{s}} \quad , \quad |1-s| < 1 \tag{3.44}$$

$$= \frac{1}{\sqrt{s}\{1 - 4((1-s)/4)\}}$$

$$= \sum_{n=0}^{\infty} \binom{2n}{n} \left(\frac{1-s}{4}\right)^n$$

$$= \sum_{n=0}^{\infty} \binom{2n}{n} \frac{1}{4^n} \sum_{j=0}^{n} (-s)^j$$

$$= \sum_{j=0}^{\infty} \sum_{n=j}^{\infty} \binom{2n}{n} \frac{1}{4^n} (-s)^j$$

Here, we use the identity $\sum_{n=0}^{\infty} \binom{2n}{n} x^n = (1-4x)^{-1/2}$, $|x| < \frac{1}{4}$.

According to Bose [25], Pade rational approximants $R_{n-1,n}(s)$ and $R_{n,n}(s)$ have simple interlacing poles and zeros on the negative real axis. These two approximants corresponding to the diagonal and superdiagonal elements show the interlacement of poles and zeros on the negative real axis as shown in equations (3.37) and (3.38). A residue at each pole is positive. The rational approximants are of an irreducible form in s. Furthermore, the realization of any approximant $R_n(s)$ into the state-space description is controllable and observable.

IV. FORMULATION OF THE CLOCK NOISE MODEL AND KALMAN FILTER

A. Description of the Clock Noise Model in the State-Space Equation

First, we consider a realization of the flicker noise characteristic. From Table 1 or equation (3.32), we get an approximate rational transfer function $R_{m+n}(s)$. Here, 'm+n' corresponds to 'n' of $R_n(s)$ in Table 1 (See Chapter III.)

$$R_{m+n}(s) = \frac{b_m s^m + b_{m-1} s^{m-1} + \ldots + b_0}{a_n s^n + a_{n-1} s^{n-1} + \ldots + a_0} \tag{4.1}$$

where $a_n = 1$ when $m = n-1$, and $a_n = \frac{1}{n+1}$ when $m = n$.

The output of $R_{m+n}(s)$ has an approximate flicker noise characteristic, when the input is a white noise. It is assumed that the order m of the numerator polynomial is chosen equal to n-1 in order for the output variance not to become infinite [3]. Then, $m+n = 2n-1$. It implies that $R_{2n-1}(s)$ becomes a proper rational transfer function. The order of the denominator of $R_{2n-1}(s)$ becomes $[\ \frac{m+n+1}{2}\ ] = n$ as shown in equation (3.35).

Studies have been done to realize the above rational transfer function into a state-space dynamic equation. Many ways of the realization have been known as canonical forms [18]. Among them, we will use the controllable canonical form to realize $R_{2n-1}(s)$.

Let an input white noise be $w_{-1}(t)$, output $y(t)$, and the internal states of the system in the state-space equation be $x_i(t)$'s, $i = 1, 2, \ldots, n$. Then, the state-space equation takes the form of the following matrix equation.

$$\begin{bmatrix} \dot{x}_1 \\ \dot{x}_2 \\ \cdot \\ \cdot \\ \cdot \\ \dot{x}_n \end{bmatrix} = \begin{bmatrix} 0 & 1 & 0 & 0 & \ldots & 0 \\ 0 & 0 & 1 & 0 & \ldots & 0 \\ 0 & 0 & 0 & 1 & \ldots & 0 \\ 0 & 0 & 0 & & . & \\ 0 & 0 & 0 & & . & 1 \\ -a_0 & -a_1 & -a_2 & & \ldots & -a_{n-1} \end{bmatrix} \begin{bmatrix} x_1 \\ x_2 \\ x_3 \\ . \\ . \\ x_n \end{bmatrix} + \begin{bmatrix} 0 \\ 0 \\ 0 \\ . \\ . \\ 1 \end{bmatrix} w_{-1}(t) \qquad (4.2)$$

And the output flicker noise is

$$y(t) = [\, b_0 \; b_1 \; \ldots \; b_{n-1} \,]\, \underline{x} \qquad (4.3)$$

The output $y(t)$ gives the same flicker noise characteristic as $R_{2n-1}(s)$ does.

Combining the white noise and random-walk noise components with the flicker noise approximation given in equation (4.2), we obtain (n+2) dimensional state-space dynamic equation. See Figure 7. Define state variables as follows: $x_1(t)$ = clock phase noise $\phi(t)$, $x_2(t)$ = random-walk frequency noise, and $x_3(t), \ldots, x_{n+2}(t)$ representing states of the flicker noise part. Then, the state-space equation is given as follows:

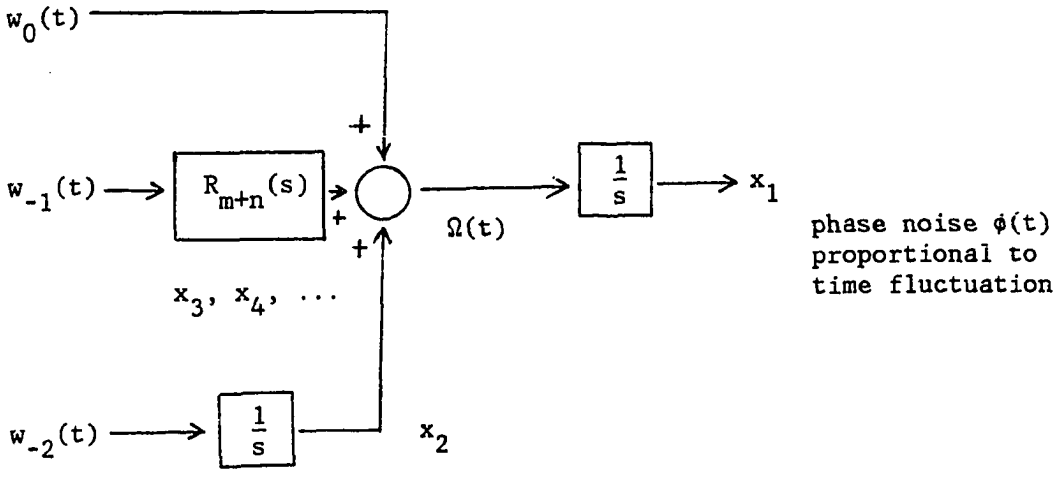

FIGURE 7. Block diagram of the clock noise model

$$\begin{bmatrix} \dot{x}_1 \\ \dot{x}_2 \\ \dot{x}_3 \\ \vdots \\ \dot{x}_{n+1} \\ \dot{x}_{n+2} \end{bmatrix} = \begin{bmatrix} 0 & 1 & b_0 & b_1 & \cdots & b_{n-1} \\ 0 & 0 & 0 & 0 & \cdots & 0 \\ 0 & 0 & 0 & 1 & \cdots & 0 \\ & & \vdots & & & \\ 0 & 0 & 0 & 0 & \cdots & 1 \\ 0 & 0 & -a_0 & -a_1 & \cdots & -a_{n-1} \end{bmatrix} \begin{bmatrix} x_1 \\ x_2 \\ x_3 \\ \vdots \\ x_{n+1} \\ x_{n+2} \end{bmatrix} + \begin{bmatrix} w_0(t) \\ w_{-2}(t) \\ 0 \\ \vdots \\ 0 \\ w_{-1}(t) \end{bmatrix}$$

Or

$$\dot{\underline{x}} = A\underline{x} + \underline{W} \tag{4.4}$$

And the output y is

$$y(t) = [\ 1\ 0\ \ldots\ 0\ ]\ \underline{x} \tag{4.5}$$

Let us examine eigenvalues of the system first. To find them, form an algebraic equation.

$$\begin{aligned} \det\ [\lambda I - A] &= \lambda^2(\lambda^n + a_{n-1}\lambda^{n-1} + \ldots + a_0) \\ &= \lambda^2 F(\lambda) \\ &= 0 \end{aligned} \tag{4.6}$$

The eigenvalue at $\lambda = 0$ with multiplicity two is due to two integrators in the system. The other eigenvalues of $F(\lambda) = 0$ are from the flicker noise modeling. It was mentioned in the previous section that roots of the denominator polynomial in any Pade table entry are all distinct: so are the roots of $F(\lambda) = 0$. See Table 2. Thus, with λ_i's such that $F(\lambda_i) = 0$, $i = 1, 2, \ldots, n$, we have

$$\begin{aligned} F(\lambda) &= \lambda^n + a_{n-1}\lambda^{n-1} + \ldots + a_0 \\ &= (\lambda+\lambda_1)(\lambda+\lambda_2)\ \ldots\ (\lambda+\lambda_n) \end{aligned} \tag{4.7}$$

Because of this distinctness it is better to reorganize the system and make the system decoupled. To do so, we start from the rational transfer function again. The transfer function in equation (4.1) is rewritten by the partial fraction expansion into a sum of terms of a form $\frac{1}{s+\lambda_i}$ so that the system is of a parallel structure. Let K_i be a gain factor corresponding to a $\frac{1}{s+\lambda_i}$ block. Then, we have a block diagram as shown in Figure 8.

The advantage for doing this is twofold. First, the system configuration becomes less sophisticated. State variables may be assigned easily according to the size of eigenvalues. Secondly, we may delete some state vectors which have very large or small time constants and thus they are negligible in the overall system performance in a certain period of time. Or we can identify important system modes and understand the system better. Hence, the dimensional reduction of the system may be easily achieved.

From Figure 8, we have a new state-space dynamic equation.

$$\dot{\underline{x}} = \begin{bmatrix} 0 & 1 & 1 & 1 & \dots & 1 \\ 0 & 0 & 0 & 0 & \dots & 0 \\ 0 & 0 & -\lambda_1 & 0 & \dots & 0 \\ 0 & 0 & 0 & -\lambda_2 & \dots & 0 \\ 0 & 0 & 0 & 0 & . & 0 \\ 0 & 0 & 0 & 0 & . & 0 \\ 0 & 0 & 0 & 0 & \dots & -\lambda_n \end{bmatrix} \underline{x} + \begin{bmatrix} w_0 \\ w_{-2} \\ K_1 w_{-1} \\ . \\ . \\ . \\ K_n w_{-1} \end{bmatrix} \tag{4.8}$$

And the output y is given by

$$y = [\ 1\ 0\ \dots\ 0\ ]\ \underline{x} \tag{4.9}$$

where $\underline{x} = [\ x_1\ \ x_2\ \ \dots\ \ x_{n+2}\ ]^T$

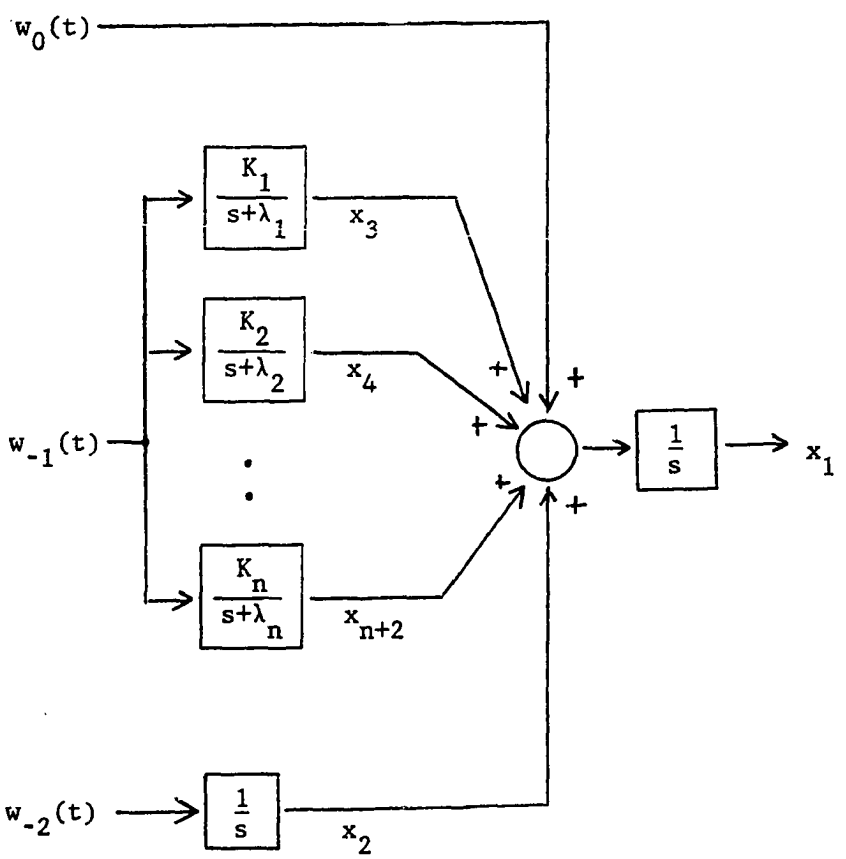

FIGURE 8. Block diagram of parallel realization of clock noise model

B. Formulation of Kalman Filter and its Parameters

We start from the system equation obtained in the previous section.

$$\dot{\underline{x}}(t) = A\underline{x}(t) + \underline{W}(t) \tag{4.10}$$

The solution $\underline{x}(t)$ to this differential equation is given by

$$\underline{x}(t) = \Phi(t-t_0)\underline{x}(t_0) + \int_{t_0}^{t} \Phi(t-\tau)\underline{W}(\tau)\, d\tau \tag{4.11}$$

where $\Phi(t)$ is the state transition matrix of the system and t_0 is a starting time.

For (n+2) dimensional system, $\Phi(t)$ is given as follows:

$$\Phi(t) = L^{-1}\,[sI-A]^{-1} \tag{4.12}$$

$$= L^{-1}\begin{bmatrix} s & -1 & -1 & -1 & \cdots & -1 \\ 0 & s & 0 & 0 & \cdots & 0 \\ 0 & 0 & s+\lambda_1 & 0 & \cdots & 0 \\ 0 & 0 & 0 & s+\lambda_2 & \cdots & 0 \\ 0 & 0 & 0 & 0 & \cdots & 0 \\ 0 & 0 & 0 & 0 & \cdots & s+\lambda_n \end{bmatrix}^{-1}$$

where L^{-1} denotes an inverse Laplace transform.

Using a matrix inversion identity [27], we get

$$\Phi(t) = \begin{bmatrix} 1 & t & \frac{1}{\lambda_1}(1-e^{-\lambda_1 t}) & \frac{1}{\lambda_2}(1-e^{-\lambda_2 t}) & \cdots & \frac{1}{\lambda_n}(1-e^{-\lambda_n t}) \\ 0 & 1 & 0 & 0 & \cdots & 0 \\ 0 & 0 & e^{-\lambda_1 t} & 0 & \cdots & 0 \\ 0 & 0 & 0 & e^{-\lambda_2 t} & \cdots & 0 \\ 0 & 0 & 0 & 0 & \cdots & 0 \\ 0 & 0 & 0 & 0 & \cdots & e^{-\lambda_n t} \end{bmatrix}$$

Since the Kalman filter usually takes a discrete form, equation (4.11) is discretized. At time $t_{k+1} = (k+1)\Delta t$, with Δt = time increment, $\underline{x}(t_{k+1})$ becomes

$$\underline{x}(t_{k+1}) = \Phi(t_{k+1} - t_k)\underline{x} + \int_{t_k}^{t_{k+1}} \Phi(t_{k+1} - \tau)\underline{W}(\tau)\, d\tau$$

$$= \Phi(\Delta t)\underline{x}(t_k) + \int_{t_k}^{t_{k+1}} \Phi(t_{k+1} - \tau)\underline{W}(\tau)\, d\tau \qquad (4.13)$$

In short, we have

$$\underline{x}_{k+1} = \Phi\underline{x}_k + \underline{w}_k \qquad (4.14)$$

$$y_k = H\underline{x}_k \qquad (4.15)$$

where $\underline{w}_k$ is defined as follows:

$$\underline{w}_k = \int_{t_k}^{t_{k+1}} \Phi(t_{k+1} - \tau)\underline{W}(\tau)\, d\tau \qquad (4.16)$$

and

$$\Phi = \Phi(\Delta t) \qquad (4.17)$$

To set up the Kalman filter equations, some definitions and assumptions are necessary [3]. They are listed below.

$\underline{x}_k$ = (n+2) state vector at time t_k, k =0, 1, 2, ...

Φ = (n+2)×(n+2) state transition matrix

$\underline{w}_k$ = (n+2) white noise sequence vector with zero mean

z_k = a scalar measurement at time t_k

v_k = a scalar measurement error with zero mean which is a white noise sequence and uncorrelated with w_k .

Then, the covariance matrix for w_k is

$$E\,[\underline{w}_k \underline{w}_i^T] = \begin{cases} Q_k & , i = k \\ 0 & , i \neq k \end{cases} \tag{4.18}$$

where T is a transposition. The covariance matrix for v_k is

$$E\,[v_k v_i^T] = \begin{cases} R_k & , i = k \\ 0 & , i \neq k \end{cases} \tag{4.19}$$

And the uncorrelatedness between $\underline{w}_k$ and v_i is assumed so that

$$E\,[\underline{w}_k v_i^T] = 0 \quad , \text{for all } i,\ k > 0 \tag{4.20}$$

With these definitions and assumptions, define an error $\underline{e}_k$ between the state $\underline{x}_k$ and its estimate $\overset{*}{\underline{x}}_k$. For convenience, drop bar signs in the vectors $\underline{x}_k$ and $\underline{w}_k$. Then,

$$e_k = x_k - \overset{*}{x}_k \tag{4.21}$$

The error covariance matrix P_k is given by

$$P_k = E\,[e_k e_k^T] \tag{4.22}$$
$$= E\,[(x_k - \overset{*}{x}_k)(x_k - \overset{*}{x}_k)^T]$$

Based upon the definitions above, the Kalman equations are given below without any derivation. For detail, see reference [3].

$$\text{Kalman gain : } K_k = \bar{P}_k H^T (H\bar{P}_k H^T + R_k)^{-1} \tag{4.23}$$

$$\text{State estimate : } \overset{*}{x}_k = \bar{x}_k + K_k\,(z_k - H\bar{x}_k) \tag{4.24}$$

$$\text{Error covariance : } P_k = (I - K_k H)\bar{P}_k (I - K_k H)^T - K_k R_k K_k^T \tag{4.25}$$

$$\text{Projection ahead : } \bar{x}_{k+1} = \Phi \overset{*}{x}_k \tag{4.26}$$

$$\bar{P}_{k+1} = \Phi P_k \Phi^T + Q_k \tag{4.27}$$

where a super minus denotes 'a priori' information.

The covariance for w_k, Q_k, is calculated by

$$Q_k = E\,[w_k w_k^T] \tag{4.28}$$
$$= E\,[\{ \int_{t_k}^{t_{k+1}} \Phi(t_{k+1} - u) W(u)\, du \}\{ \int_{t_k}^{t_{k+1}} \Phi(t_{k+1} - v) W(v)\, dv \}^T]$$
$$= \int_{t_k}^{t_{k+1}} \Phi(t_{k+1} - u)\, E\,[\, W(u) W^T(v)\,]\, \Phi^T(t_{k+1} - v)\, du\, dv$$

From equation (4.28), define W' as follows:

$$E\,[\, W(u) W^T(v)\,] = W' \delta(u - v) \tag{4.29}$$

where W' is given by

$$W' = \left[\begin{array}{cc|ccc} S_w & 0 & & & \\ 0 & S_r & & 0 & \\ \hline & & K_1^2 S_f & K_1 K_2 S_f & \cdots \quad K_1 K_n S_f \\ & 0 & K_1 K_2 S_f & K_2^2 S_f & \cdots \quad K_2 K_n S_f \\ & & \cdot & & \cdots \quad \cdot \\ & & K_1 K_n S_f & & \cdots \quad K_n^2 S_f \end{array}\right]$$

where S_w, S_f, and S_r denote spectral amplitudes for white, flicker, and random-walk noise, respectively, as defined in Chapter I.

Then, we have

$$Q_k = \int_{t_k}^{t_{k+1}} \Phi(t_{k+1} - u) W' \Phi^T(t_{k+1} - u)\, du \tag{4.30}$$

Setting $t_{k+1} - u = t$ and $t_{k+1} - t_k = \Delta t$, we get

$$Q_k = \int_0^{\Delta t} \Phi(t) W' \Phi^T(t)\, dt$$

After carrying out manipulation, we have

$$Q_k = \begin{array}{c} \begin{array}{cc} 2 & n \text{ columns} \end{array} \\ \left[\begin{array}{cc} Q_A & Q_B \\ Q_B^T & Q_D \end{array}\right] \begin{array}{l} 2 \text{ rows} \\ n \text{ rows} \end{array} \end{array} \tag{4.31}$$

where $Q_A \in R^{(2\times 2)}$, $Q_B \in R^{(2\times n)}$, and $Q_D \in R^{(n\times n)}$

Each entry of the Q matrix is given by

$$Q_{A,11} = S_w \Delta t + \sum_{i=1}^{n} \sum_{j=1}^{n} \frac{K_i K_j}{\lambda_i \lambda_j} \{\Delta t - \frac{1-e^{-\lambda_i \Delta t}}{\lambda_i} - \frac{1-e^{-\lambda_j \Delta t}}{\lambda_j} + \frac{1-e^{-(\lambda_i+\lambda_j)\Delta t}}{\lambda_i+\lambda_j}\} S_f + S_r \frac{1}{3}(\Delta t)^3$$

$$Q_{A,12} = S_r \frac{1}{2}(\Delta t)^2$$

$$Q_{A,22} = S_r \Delta t$$

$$Q_{B,1j} = \sum_{i=1}^{n} \frac{1}{\lambda_i} \{ \frac{1-e^{-\lambda_j \Delta t}}{\lambda_j} - \frac{1-e^{-(\lambda_i+\lambda_j)\Delta t}}{\lambda_i+\lambda_j} \} K_i K_j S_f$$

$$Q_{B,2j} = 0$$

$$Q_{D,ij} = K_i K_j \frac{1-e^{-(\lambda_i+\lambda_j)\Delta t}}{\lambda_i+\lambda_j} S_f$$

Note that we can obtain an exact expression for Q_{k11} of Q_k by using a method shown in the equation (5.3.14) of reference [3]. From the transfer function diagram (Figure 7), we get $x_1(t)$ as follows:

$$x_1(t) = w_0(t) * u(t) + w_{-1}(t) * 2\sqrt{(\frac{t}{\pi})} + w_{-2}(t) * t \qquad (4.32)$$

$$= \int_0^t w_0(t-u)\, du + 2 \int_0^t \sqrt{(\frac{t-u}{\pi})}\, w_{-1}(u)\, du + \int_0^t (t-u) w_{-2}(u)\, du$$

where u(t) is a unit-step function.

Then, Q_{k11} is given by

$$Q_{k11} = E\ [\ x_1^2(t)\ ]_{\ t=\Delta t}$$

And

$$E\ [\ x_1^2(t)\ ] = \int_0^t \int_0^t S_w\ \delta(u-v)\ du\ dv$$

$$+ \frac{4}{\pi} \int_0^t \int_0^t \sqrt{((t-u)(t-v))}\ S_f\ \delta(u-v)\ du\ dv$$

$$+ \int_0^t \int_0^t S_r\ (t-u)(t-v)\ du\ dv$$

$$= \int_0^t S_w\ du + \frac{2}{\pi} \int_0^t (t-u)\ S_f\ du + \int_0^t S_r\ (t-u)^2\ du$$

$$= S_w t + \frac{2}{\pi} S_f\ t^2 + S_r\ \frac{1}{3}\ t^3$$

Therefore,

$$Q_{k11} = S_w \Delta t + \frac{2}{\pi} S_f (\Delta t)^2 + S_r\ \frac{1}{3} (\Delta t)^3 \qquad (4.33)$$

Comparing equation (4.31) to equation (4.33), it shows that the former is just an approximation of the latter, especially the second term due to the flicker noise. In the former, the result is derived from the finite dimensional system, while the latter is directly obtained from the original flicker noise process. R_k can be determined by considering the measuring equipment accuracies and environmental conditions.

C. Error Analysis and Suboptimal Filtering

In this section, our objective is to study the error accumulation in the clock noise model. To do so, two types of error analysis methods are commonly used - Monte Carlo simulation and linear error analysis [3,28,29]. In a Monte Carlo simulation, the effect of the nonlinearities on the filter errors and the effects of approximations in the filter equations are determined. But it requires a large number of simulations to determine the error statistics. In a linear error analysis, the Kalman filter equations are used to propagate the error covariance along with state estimates. It is an advantage that only one computer run is necessary to get the desired error statistic. It is more economical than the Monte Carlo method in the light of computer run-time and/or in a real-time operation. Since we have developed the Kalman filter equations in the previous section, we will use the second method for the study of the error statistics. It was shown that the error covariance matrix can be propagated without forming state estimates in the Kalman filter equations [3]. Hence, less steps can be taken in the loop of the Kalman filter equations by skipping steps of the state estimation. Refer to Figure 9.

However, because of the presence of the flicker noise and its odd power processes the ideal clock noise processes are only expressed by an infinite number of state variables. The finite dimensional state-space equation is far from a true model for the clock noise processes. Thus, the Kalman filter may be non-optimum in the sense of least square error, even though it may be regarded optimum in our finite dimensional state-

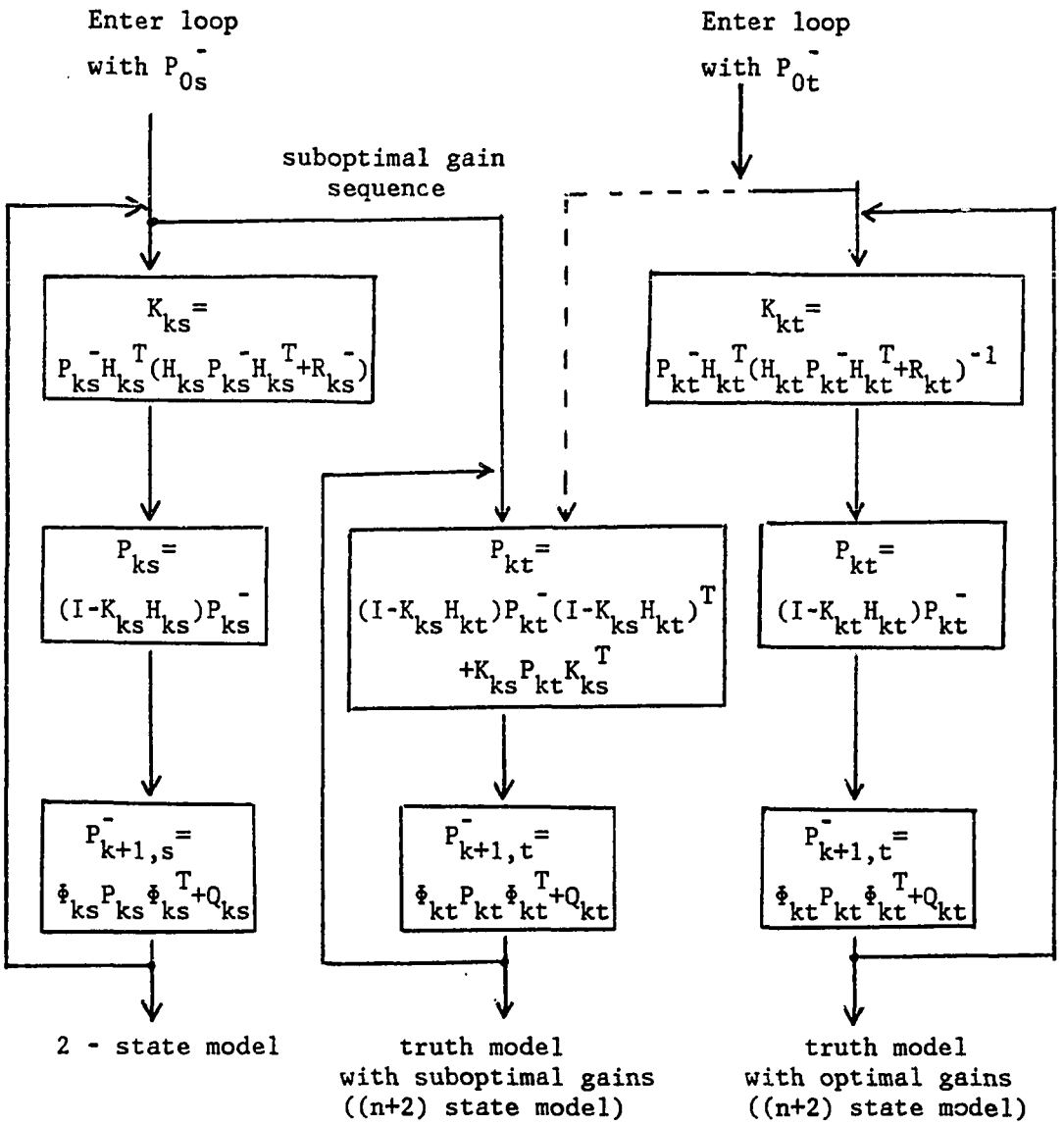

FIGURE 9. Recursive loop for suboptimal error analysis

space equation. It is just an approximation with (n+2) dimensions to the ideal one. If accurate behavior of the flicker noise is essential, then the dimension n must be very large to closely imitate the flicker noise process. To accomplish this, the dimension of the matrix in the Kalman filter equations becomes so large that the real-time operation may be extremely difficult or impossible due to a heavy computational burden.

Let us call this (n+2) dimensional filter a truth model even if it does not mean a true model in a strict sense. The terminology "truth model" is common in the Kalman filtering [3,30]. Sometimes it is wise to consider a subset of the system components by selectively choosing state vectors and thus reduce the dimensionality of the overall system. It is called a suboptimal filter (or a reduced order filter) [3,29,30] with less dimension than the (n+2) dimension of the linear optimum filter. The suboptimal filter is formed by retaining the state vectors which represent significant modes of the system and discarding less significant ones. In our case, the first two state vectors are chosen in the state-space equations (4.14) through (4.33).

That is

$$\begin{bmatrix} \dot{x}_1 \\ \dot{x}_2 \end{bmatrix} = \begin{bmatrix} 0 & 1 \\ 0 & 0 \end{bmatrix} \begin{bmatrix} x_1 \\ x_2 \end{bmatrix} + \begin{bmatrix} w_1 \\ w_2 \end{bmatrix} \tag{4.34}$$

$$y = [\, 1 \quad 0 \,]\, \underline{x} \tag{4.35}$$

As mentioned earlier, the random-walk noise is more divergent than the flicker noise. Actually, the flicker noise is logarithmically divergent [13] as discussed in the Chapter II. Since we are interested in the long-term behavior of clock error due to these noise processes, the above facts can be utilized to choose noise components, w_1 and w_2, properly. The white noise may be retained to represent instantaneous fluctuations in the system. Based on the above discussion, hence, only the white and random-walk noises may be considered excluding the flicker noise whose characteristic is in between the other two. We will consider this further in next chapter.

To assess an error in the suboptimal filter, the truth model Kalman filter is run with suboptimal gains. See the procedure in Figure 9. In Figure 9, the optimal gain is a gain matrix of the truth model Kalman filter. And the suboptimal gain is a gain matrix of the two state suboptimal Kalman filter. If the suboptimal and truth model filters are running together in parallel, we can obtain a good comparison of the error propagation and determine whether the presence of the flicker noise is important or not. If it turns out that the flicker noise does not affect the error propagation much compared to others, then it may provide a good justification to ignore it in the suboptimal filtering. And the suboptimal filter may be used in real applications. See the different suboptimal mechanization in reference [31,36].

D. Analysis of Optimal Prediction Error by the Bode-Shannon Method

Optimal prediction error for the clock phase error which corresponds to the time fluctuations $x_1(t)$ in the Kalman filter equations can be obtained by predicting N steps ahead of the projection [3,32]. That is

$$P(k+N|k) = \Phi_{k+N,k} P(k|k) \Phi^T_{k+N,k} + Q_{k+N,k} \tag{4.36}$$

where

$P(k+N|k)$ = error covariance associated with $\overset{*}{x}(k+N|k)$

$\Phi_{k+N,k}$ = state transition matrix for time interval from t_k to t_{k+N}

$Q_{k+N,k}$ = covariance of the driven response for time interval from t_k to t_{k+N}

$P(k|k)$ = filter estimate and its error covariance at t_k

If we look into the above equation, we find out that the computation of Φ and Q is needed every time when a prediction step N is changed. It is wasteful in time and storage for recomputing or storing different Φ's and Q's when the step N is changed. The Bode-Shannon method provides an alternative for this [33,34]. The optimal prediction error can be analytically obtained by the direct application of it.

In our shaping filter approach, each noise process is generated from an independent white noise source. Thus, output noises are mutually independent. The uncorrelatedness of three noise processes assures the application of the B-S method to each noise separately.

We follow the method closely for finding the optimal prediction error due to the flicker phase noise. For the other two noises - white and random-walk noises - the same procedure is applied to find the optimal prediction error. General procedure can be described as follows.

Let us consider two transfer function boxes $Y_1(s)$ and $Y_2(s)$ whose outputs are the white noise and α seconds-delayed replica of the input flicker phase noise, respectively, as shown in Figure 10. The problem is to obtain the best estimate of $f(t+\alpha)$ from $f(t)$, when there is no system perturbing noise present.

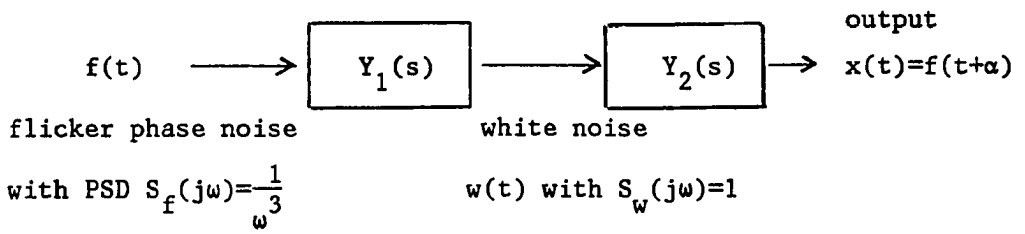

FIGURE 10. Block diagram for pure prediction problem for flicker noise

We follow the steps in the Bode-Shannon method [33,34]. First, we determine $Y_1(s)$. Let

$$Y_1(j\omega) = | Y_1(j\omega) | e^{j\Psi_1(\omega)}$$

Since

$$S_f(j\omega) \mid Y_1(j\omega) \mid^2 = 1$$

we have

$$\mid Y_1(j\omega) \mid = \frac{1}{\sqrt{S_f(j\omega)}}$$

$$= \sqrt{\omega^3} \tag{4.37}$$

And the phase-shift function of $Y_1(s)$, $\Psi_1(\omega)$ is given by

$$\Psi_1(\omega) = \frac{2\omega}{\pi} \int_0^\infty \frac{\ln \{ Y_1(jv) - Y_1(j\omega) \}}{v^2 - \omega^2} \, dv \tag{4.38}$$

$$= \frac{3\omega}{\pi} \int_0^\infty \frac{\ln v - \ln w}{v^2 - \omega^2} \, dv$$

$$= \frac{3\pi}{4}$$

Therefore,

$$Y_1(j\omega) = \sqrt{\omega^3} \; e^{j(3\pi/4)}$$

Or

$$Y_1(s) = s\sqrt{s} \tag{4.39}$$

Let K(t) be the inverse Laplace transform of $Y_1^{-1}(s)$. Then,

$$K(t) = L^{-1} [Y_1^{-1}(s)] \tag{4.40}$$

$$= L^{-1} [\frac{1}{s\sqrt{s}}]$$

$$= 2 \sqrt{(\frac{t}{\pi})}$$

Secondly, construct a filter whose impulse response is

$$K'(t) = \begin{cases} K(t+\alpha) & , \text{ for } t \geq 0 \\ 0 & , \text{ for } t < 0 \end{cases} \tag{4.41}$$

Then, the transfer function $Y_2(s)$ is defined by

$$\begin{aligned} Y_2(s) &= L^{-1} [\, K'(t) \,] \\ &= \int_0^{\infty} 2 \sqrt{\left(\frac{(t+\alpha)}{\pi}\right)}\, e^{-st}\, dt \quad , \quad \alpha > 0 \\ &= 2 \sqrt{\left(\frac{\alpha}{\pi}\right)}\, \frac{1}{s} + \frac{e^{s\alpha}}{s\sqrt{s}}\, \mathrm{erfc}(\sqrt{(s\alpha)}) \quad , \quad \alpha > 0 \end{aligned} \tag{4.42}$$

The optimal predictor then has a transfer function $Y_1(s)Y_2(s)$.

$$\begin{aligned} Y_1(s)Y_2(s) &= s\sqrt{s} \left[\, 2 \sqrt{\left(\frac{\alpha}{\pi}\right)}\, \frac{1}{s} + \frac{e^{s\alpha}}{s\sqrt{s}}\, \mathrm{erfc}(\sqrt{(s\alpha)}) \,\right] , \quad \alpha > 0 \\ &= 2 \sqrt{\left(\frac{\alpha}{\pi}\right)}\, \sqrt{s} + e^{s\alpha}\, \mathrm{erfc}(\sqrt{(s\alpha)}) \end{aligned} \tag{4.43}$$

This optimal predictor is quite complicated. It may not be useful for real applications. However, this method specifies how to find a mean square prediction error. Since the input to $Y_2(s)$ is a white noise and there is no information available for the α-second interval, the prediction error is due to the noise of this interval. Thus,

$$\begin{aligned} E [\, e_x^2 \,] &= \int_0^{\alpha} \int_0^{\alpha} K(u)\, K(v)\, \delta(u-v)\, du\, dv \\ &= \int_0^{\alpha} K^2(u)\, du \\ &= \int_0^{\alpha} 4\, \frac{u}{\pi}\, du \\ &= \frac{2\alpha^2}{\pi} \end{aligned} \tag{4.44}$$

Similarly, for the random-walk phase noise, we have

$$\text{Optimal predictor} : Y_1(s)Y_2(s) = 1 + \alpha s \tag{4.45}$$

$$\text{Prediction error} : E\left[e_x^2 \right] = \frac{1}{3}\alpha^3 \tag{4.46}$$

For the white phase noise, we have

$$\text{Optimal predictor} : Y_1(s)Y_2(s) = 1 \tag{4.47}$$

$$\text{Prediction error} : E\left[e_x^2 \right] = \alpha \tag{4.48}$$

Combining these processes with proper input noise powers, we get the optimal prediction error

$$E\left[e_x^2 \right] = S_w \alpha + S_f \frac{2}{\pi}\alpha^2 + S_r \frac{1}{3}\alpha^3 \tag{4.49}$$

From equation (4.49), we find that the prediction error is dominated by the random-walk noise as time goes on. For a long range prediction, it is sufficient to consider the random-walk noise only.

When this result is incorporated into the discrete Kalman equations, we can rewrite equation (4.49) with a step size Δt seconds and the projection ahead N steps, i.e., $\alpha = N\Delta t$.

$$E\left[e_x^2 \right] = S_w N\Delta t + S_f \frac{2}{\pi}(N\Delta t)^2 + S_r \frac{(N\Delta t)^3}{3} \tag{4.50}$$

For example, with same input powers in three noise processes and $\Delta t = 1$, the random-walk phase noise becomes 10 times bigger than the flicker phase noise after 18 steps. The result in equation (4.50) coincides with that of equation (4.33).

V. APPLICATIONS

A. Numerical Example

In this section, we compare the behavior of the truth model and 2-state suboptimal model described in the last chapter. For this, we select a 5-state truth model whose time response closely follows the flicker noise, approximately from 0.07 to 13.9 seconds, corresponding to the eigenvalues {-0.0718, -1, -13.9282} of $R_5(s)$ in Table 2. Also see Figures 4 and 5. Because of the choice of the 5-state model, choose a step size $\Delta t = 1$ which belongs to this time interval. Then, the 2-state suboptimal model is constructed from the 5-state truth model accordingly.

To program the Kalman filter recursive equations, we must first determine the filter parameter values. Since we do not have any prior knowledge about a priori estimate, $\hat{x}_0^- = 0$, we set $P_0^- = 0$ in both cases. Concerning the measuring equipment noise susceptibility, we assign an appropriate value to R_k. In this example, we choose $R_k = 0.625 \times 10^{-17}$ in both the truth and 2-state models. In order to calculate Q matrices, the parameters h_i's in Figure 11 are used. They are $h_0 = 9.43 \times 10^{-20}$, $h_{-1} = 1.8 \times 10^{-19}$, and $h_{-2} = 3.8 \times 10^{-21}$.

1. 5-state truth model

$$\begin{bmatrix} \dot{x}_1 \\ \dot{x}_2 \\ \dot{x}_3 \\ \dot{x}_4 \\ \dot{x}_5 \end{bmatrix} = \begin{bmatrix} 0 & 1 & 1 & 1 & 1 \\ 0 & 0 & 0 & 0 & 0 \\ 0 & 0 & -\lambda_1 & 0 & 0 \\ 0 & 0 & 0 & -\lambda_2 & 0 \\ 0 & 0 & 0 & 0 & -\lambda_3 \end{bmatrix} \begin{bmatrix} x_1 \\ x_2 \\ x_3 \\ x_4 \\ x_5 \end{bmatrix} + \begin{bmatrix} w_{-0} \\ w_{-2} \\ K_1 w_{-1} \\ K_2 w_{-1} \\ K_3 w_{-1} \end{bmatrix} \tag{5.1}$$

where

$$K_1 = 3.57265\times10^{-1}, \quad K_2 = \frac{2}{3}, \quad K_3 = 4.97607$$
$$\lambda_1 = 7.17967\times10^{-2}, \quad \lambda_2 = 1, \quad \lambda_3 = 13.9282$$

And the output is

$$y = [\, 1 \quad 0 \quad 0 \quad 0 \quad 0 \,]\, \underline{x} \tag{5.2}$$

State transition matrix Φ is given as follows:

$$\Phi = \begin{bmatrix} 1 & \Delta t & \frac{1}{\lambda_1}(1-e^{-\lambda_1\Delta t}) & \frac{1}{\lambda_2}(1-e^{-\lambda_2\Delta t}) & \frac{1}{\lambda_3}(1-e^{-\lambda_3\Delta t}) \\ 0 & 1 & 0 & 0 & 0 \\ 0 & 0 & e^{-\lambda_1\Delta t} & 0 & 0 \\ 0 & 0 & 0 & e^{-\lambda_2\Delta t} & 0 \\ 0 & 0 & 0 & 0 & e^{-\lambda_3\Delta t} \end{bmatrix} \tag{5.3}$$

$$= \begin{bmatrix} 1 & 1 & 0.9649 & 0.6321 & 0.0718 \\ 0 & 1 & 0 & 0 & 0 \\ 0 & 0 & 0.9307 & 0 & 0 \\ 0 & 0 & 0 & 0.3679 & 0 \\ 0 & 0 & 0 & 0 & 0.8934\times10^{-6} \end{bmatrix}$$

From equations (4.31) and (4.33), Q is given by

$$Q = \begin{bmatrix} 4.306 & 0.3747 & 1.453 & 1.611 & 0.5027 \\ 0.3747 & 0.7501 & 0 & 0 & 0 \\ 1.453 & 0 & 0.6724 & 0.8628 & 0.7231 \\ 1.611 & 0 & 0.8628 & 1.088 & 1.266 \\ 0.5027 & 0 & 0.7231 & 1.266 & 5.097 \end{bmatrix} \times 10^{-19} \qquad (5.4)$$

For computation of Q matrix, numerical values of h_i's are obtained from Figure &fig51..

a. Numerical aspects on the calculation of Φ and Q matrices

There are a few points to be mentioned for computing the Φ and Q matrices. Since the eigenvalues of the A matrix, excluding an eigenvalue at zero with double multiplicity, in equation (4.6) are widely dispersed, it is difficult to directly compute $\Phi = e^{A\Delta t}$ from a power series expansion of the exponential matrix function due to a roundoff error. Let $|\lambda_{max}|$ and $|\lambda_{min}|$ be the largest and smallest eigenvalues in magnitude, respectively, among eigenvalues λ_i. Then, if $|\frac{\lambda_{max}}{\lambda_{min}}|$ is much larger than one, the power series expansion should not be used [35].

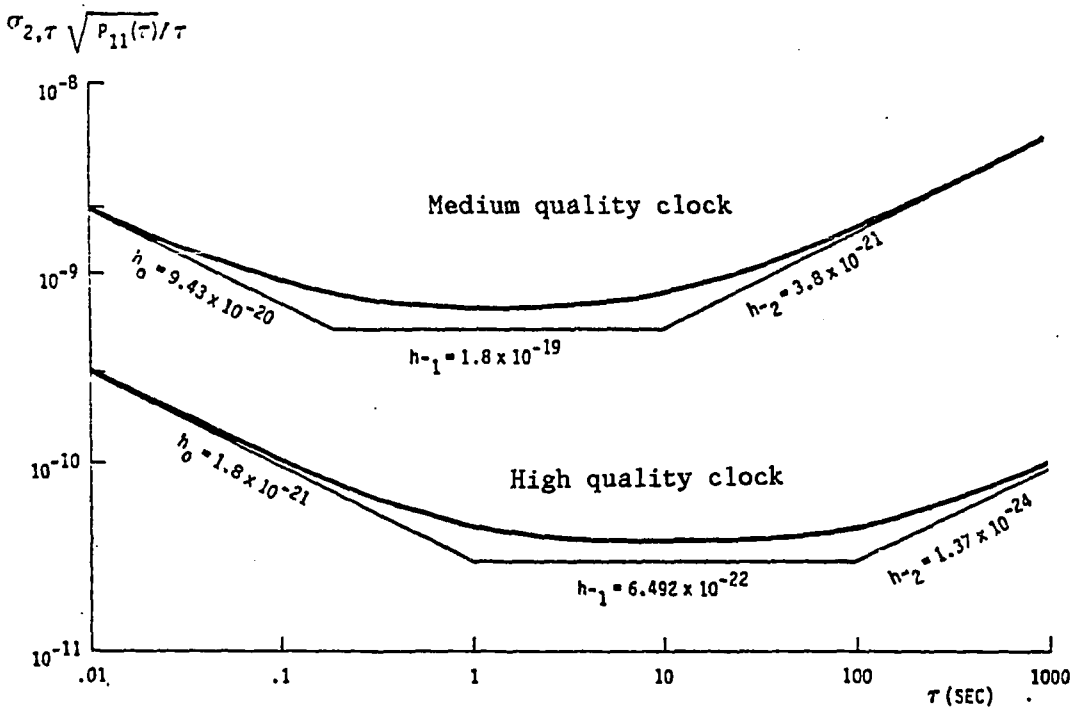

FIGURE 11. The h parameters for typical crystal oscillators (taken from reference [31])

But in our case, we have an analytic expression of Φ given by equation (4.12). It is preferable to use equation (4.12) after finding eigenvalues of the A matrix. Concerning the Q matrix, it is easier to determine the Φ and Q matrices for a tiny fraction of Δt and follow the method suggested in reference [3].

2. 2-state suboptimal model with different Q matrices

$$\begin{bmatrix} \dot{x}_1 \\ \dot{x}_2 \end{bmatrix} = \begin{bmatrix} 0 & 1 \\ 0 & 0 \end{bmatrix} \begin{bmatrix} x_1 \\ x_2 \end{bmatrix} + \begin{bmatrix} w_1 \\ w_2 \end{bmatrix} \tag{5.5}$$

The output y is

$$y = [\ 1 \quad 0\ ]\ \underline{x} \tag{5.6}$$

Then, the state transition matrix Φ is given by

$$\Phi = \begin{bmatrix} 1 & \Delta t \\ 0 & 1 \end{bmatrix} \tag{5.7}$$

$$= \begin{bmatrix} 1 & 1 \\ 0 & 1 \end{bmatrix}$$

Determination of the Q matrix in the 2-state suboptimal filter is crucial to closely follow the behavior of the truth model. We will consider four candidates for the Q matrix and then look at the clock error propagation in the suboptimal filter. This will aid in the selection of a proper Q matrix which best fits the suboptimal model.

Four candidates for the Q matrix are chosen as follows:

1. We adopt the upper left (2×2) elements of the 5-state Q matrix. From equation (4.31), we have

$$Q = \begin{bmatrix} S_w\Delta t + \frac{2}{\pi}S_f(\Delta t)^2 + \frac{1}{3}S_r(\Delta t)^3 & \frac{1}{2}S_r(\Delta t)^2 \\ \frac{1}{2}S_r(\Delta t)^2 & S_r\Delta t \end{bmatrix} \tag{5.8}$$

$$= \begin{bmatrix} \frac{1}{2}h_0\Delta t+2h_{-1}(\Delta t)^2+\frac{1}{3}2\pi^2h_{-2}(\Delta t)^3 & \pi^2h_{-2}(\Delta t)^2 \\ \pi^2h_{-2}(\Delta t)^2 & 2\pi^2h_{-2}\Delta t \end{bmatrix}$$

$$= \begin{bmatrix} 4.306 & 0.3747 \\ 0.3747 & 0.7501 \end{bmatrix} \times 10^{-19}$$

2. The second candidate is obtained by deleting a flicker noise component, since it is less divergent than a random-walk noise and usually complex to represent. Then, the Q matrix does not contain any term related to the flicker noise.

$$Q = \begin{bmatrix} S_w\Delta t+\frac{1}{3}S_r(\Delta t)^3 & \frac{1}{2}S_r(\Delta t)^2 \\ \frac{1}{2}S_r(\Delta t)^2 & S_r\Delta t \end{bmatrix} \tag{5.9}$$

$$= \begin{bmatrix} \frac{1}{2}h_0\Delta t+\frac{1}{3}2\pi^2h_{-2}(\Delta t)^3 & \pi^2h_{-2}(\Delta t)^2 \\ \pi^2h_{-2}(\Delta t)^2 & 2\pi^2h_{-2}\Delta t \end{bmatrix}$$

$$= \begin{bmatrix} 0.7215 & 0.3747 \\ 0.3747 & 0.7501 \end{bmatrix} \times 10^{-19}$$

3. In reference [31], a different Q matrix is suggested for the same 2-state suboptimal model.

$$Q = \begin{bmatrix} \frac{1}{2}h_0\Delta t+2h_{-1}(\Delta t)^2+\frac{1}{3}2\pi^2h_{-2}(\Delta t)^3 & 2h_{-1}\Delta t+\pi^2h_{-2}(\Delta t)^2 \\ 2h_{-1}\Delta t+\pi^2h_{-2}(\Delta t)^2 & \frac{1}{2\Delta t}h_0+2h_{-1}+\frac{8}{3}\pi^2h_{-2}\Delta t \end{bmatrix} \quad (5.10)$$

$$= \begin{bmatrix} 4.322 & 3.975 \\ 3.975 & 5.072 \end{bmatrix} \times 10^{-19}$$

4. In reference [36], another form of the Q matrix is reported. It is given by

$$Q = \begin{bmatrix} \frac{1}{2}h_0\Delta t+2h_{-1}(\Delta t)^2+\frac{1}{3}2\pi^2h_{-2}(\Delta t)^3 & 2h_{-1}\Delta t+\pi^2h_{-2}(\Delta t)^2 \\ 2h_{-1}\Delta t+\pi^2h_{-2}(\Delta t)^2 & 2\pi^2h_{-2}\Delta t \end{bmatrix} \quad (5.11)$$

$$= \begin{bmatrix} 4.322 & 3.975 \\ 3.975 & 0.7501 \end{bmatrix} \times 10^{-19}$$

With these different Q matrices, Kalman filters of the 5-state and 2-state suboptimal models are run in parallel. See Figure 9 for the suboptimal error analysis.

3. Discussion

Estimation error standard deviations for 170 steps have been plotted in Figure 12. From t = 0 to t = 49Δt with step size Δt = 1, it is assumed that no measurement is available for a 'free running' purpose. From t = 50Δt to t = 69Δt, measurement starts for estimation and R_k is set to 0.625×10^{-17}. It shows that, after several steps, the standard deviations rapidly converge to a constant value. At t = 70Δt, filters are again in the free running mode for the next 100 steps.

From Figure 12, we may say that every candidate of the 2-state suboptimal model shows no big departure from the 5-state truth model except the third one among four Q matrix candidates. The third one is slightly larger, but not noticeable in the plot. This is expected since Q_{11} of the Q matrix has the same formula as each candidate. In Figure 13, the suboptimal error analysis is performed with 6th order (6-state truth) model. This consistently agrees with results of the 5-state truth model.

Prediction error standard deviations of both the 5th and 6th order truth models do not show much departure from each other in case of time step size Δt= 1. See Figures 14 and 15. Deviation of prediction errors from the optimal one obtained by the Bode-Shannon method is about 30 % greater at the prediction of 80 steps. Table 4 gives the RMS prediction error comparison between the 5th and 6th order truth models.

In the Q matrices for the 2-state model, all candidates except the third have same prediction errors and closely follow the truth model as

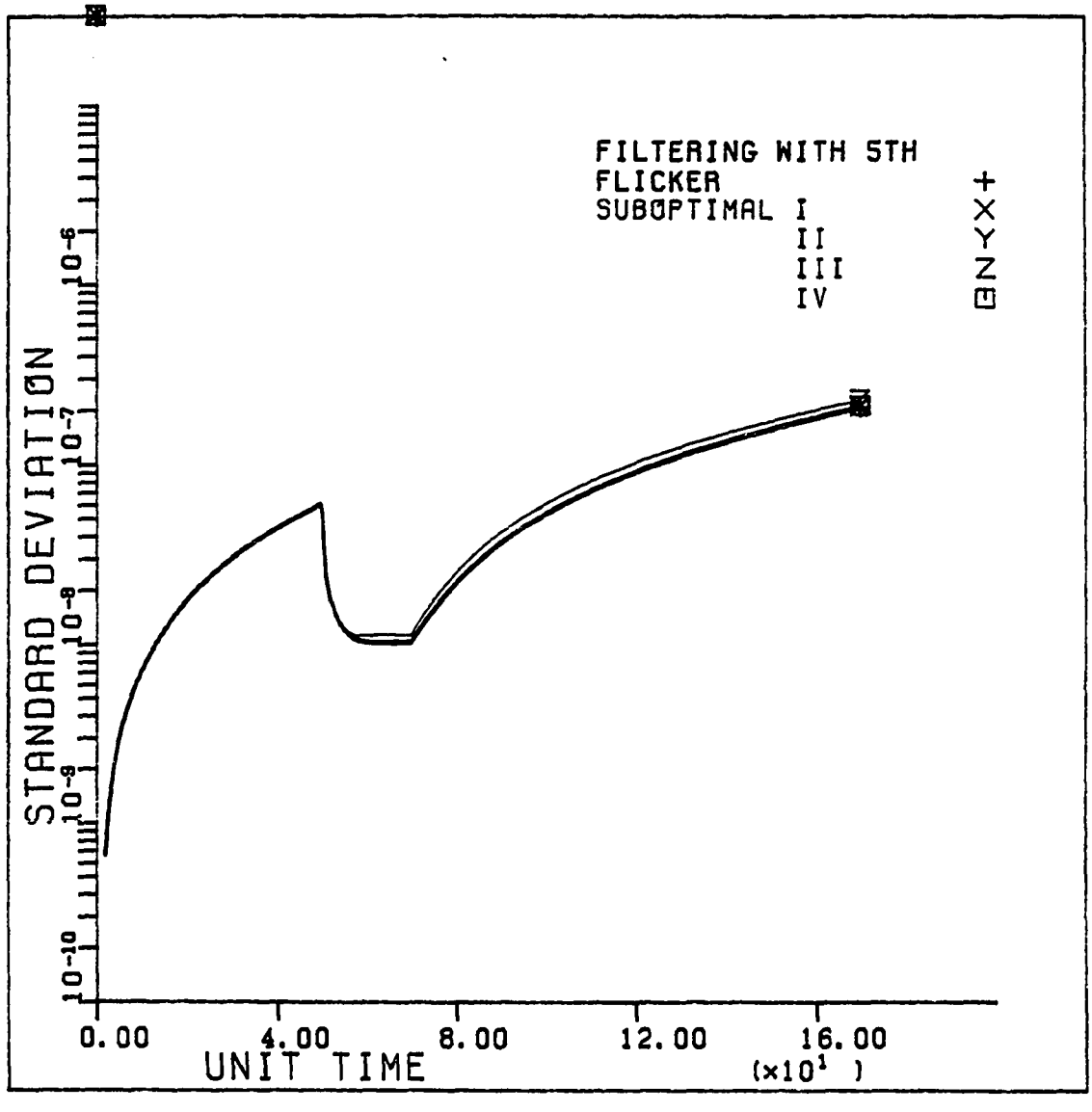

FIGURE 12. Suboptimal error analysis with 5th order model (estimation)

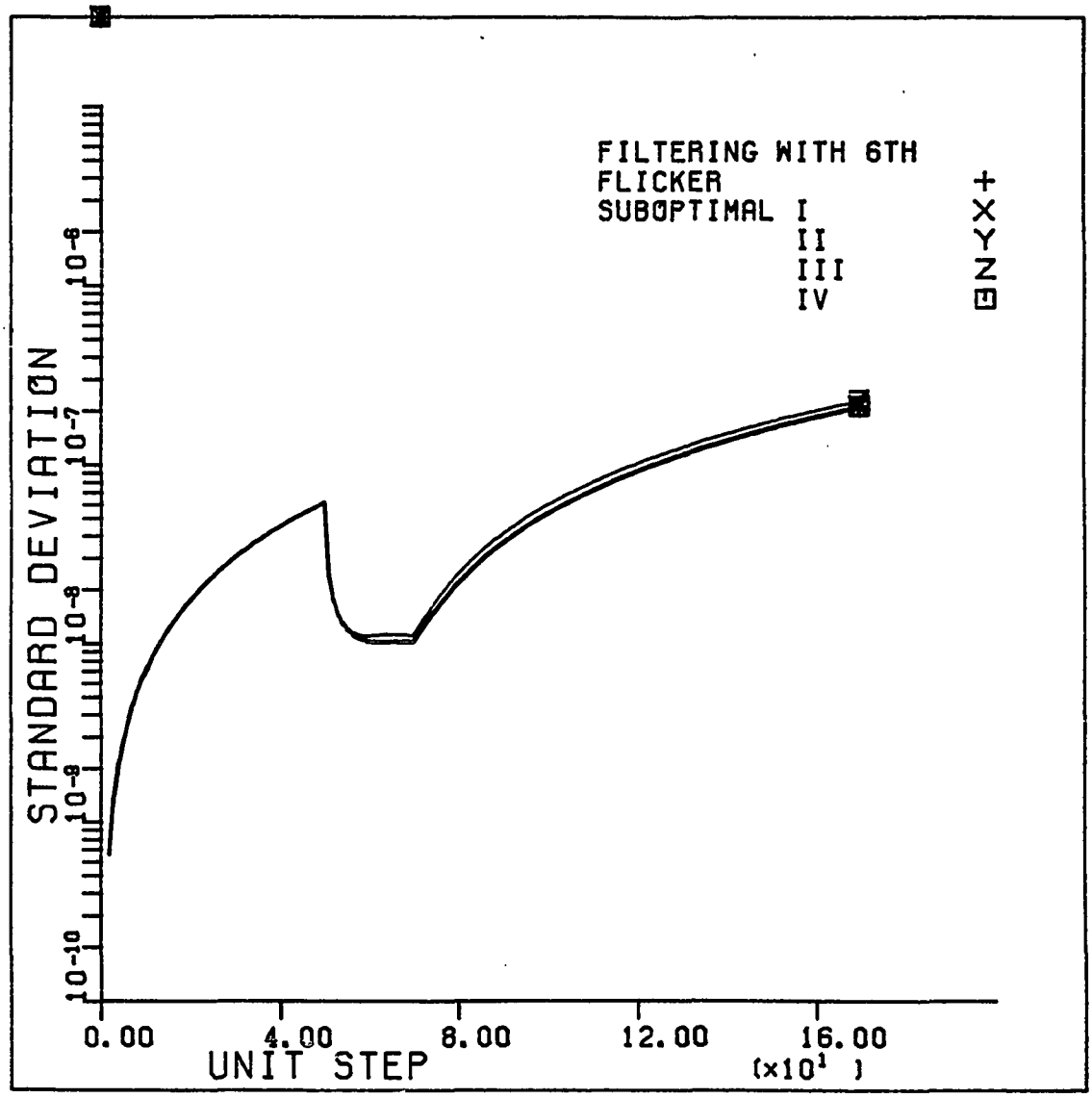

FIGURE 13. Suboptimal error analysis with 6th order model (estimation)

TABLE 4. Comparison between the 5th and 6th order models for prediction

Time lapse (steps)	5th order	6th order
10	0.2153×10^{-7}	0.2146×10^{-7}
20	0.3606×10^{-7}	0.3598×10^{-7}
30	0.5273×10^{-7}	0.5263×10^{-7}
40	0.7120×10^{-7}	0.7302×10^{-7}
50	0.9124×10^{-7}	0.9114×10^{-7}
60	0.1127×10^{-6}	0.1126×10^{-6}
70	0.1354×10^{-6}	0.1355×10^{-6}
80	0.1594×10^{-6}	0.1596×10^{-6}

in the estimation case. In the third candidate, the prediction error becomes slightly larger than any others after 80 steps. Only in the second candidate, the prediction error is slightly less because of the absence of the flicker noise component in the Q matrix. This tells us that the long-term effect due to the flicker noise is negligible in most cases ($t \geq 1$).

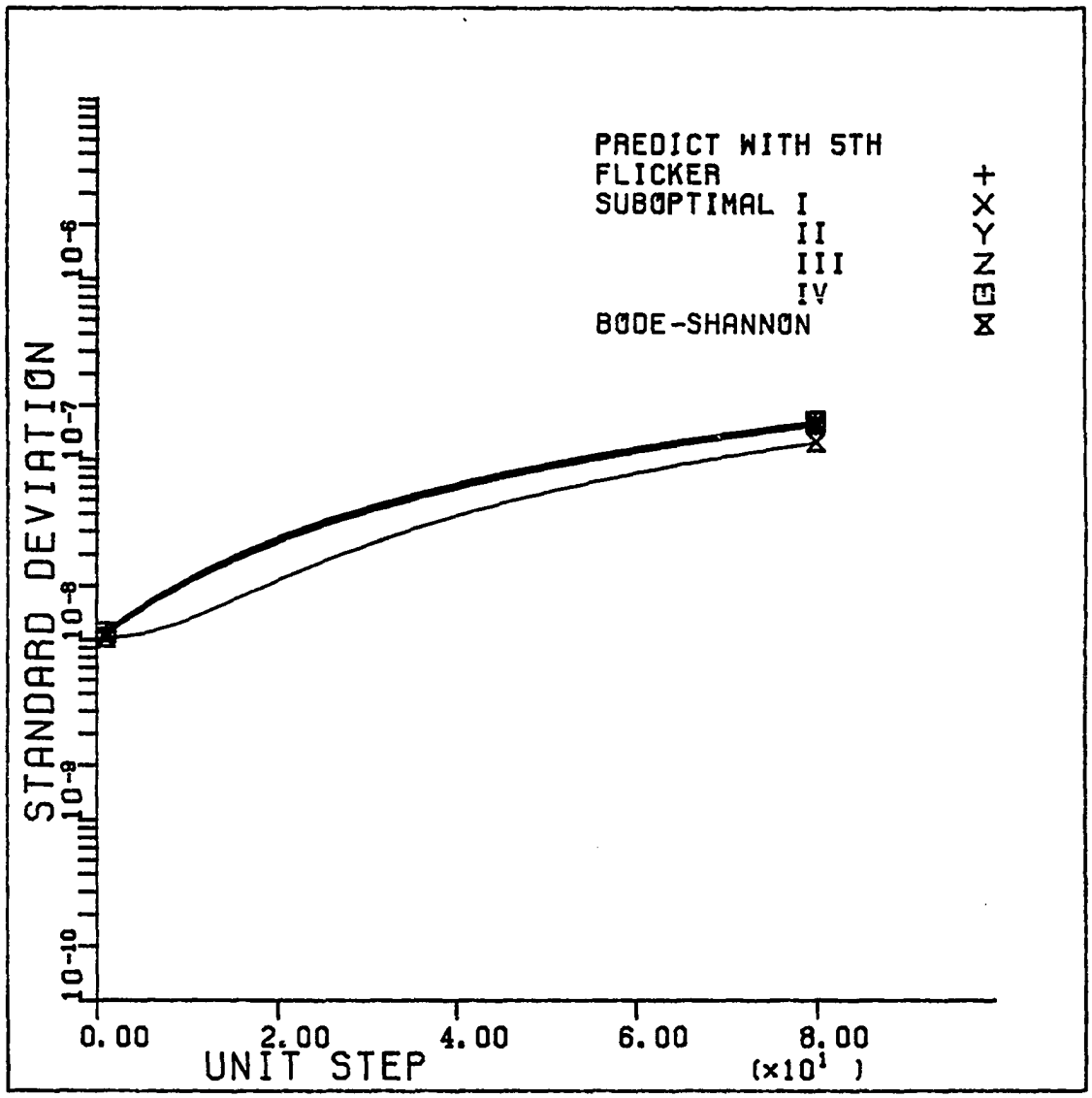

FIGURE 14. Suboptimal error analysis with 5th order model (prediction)

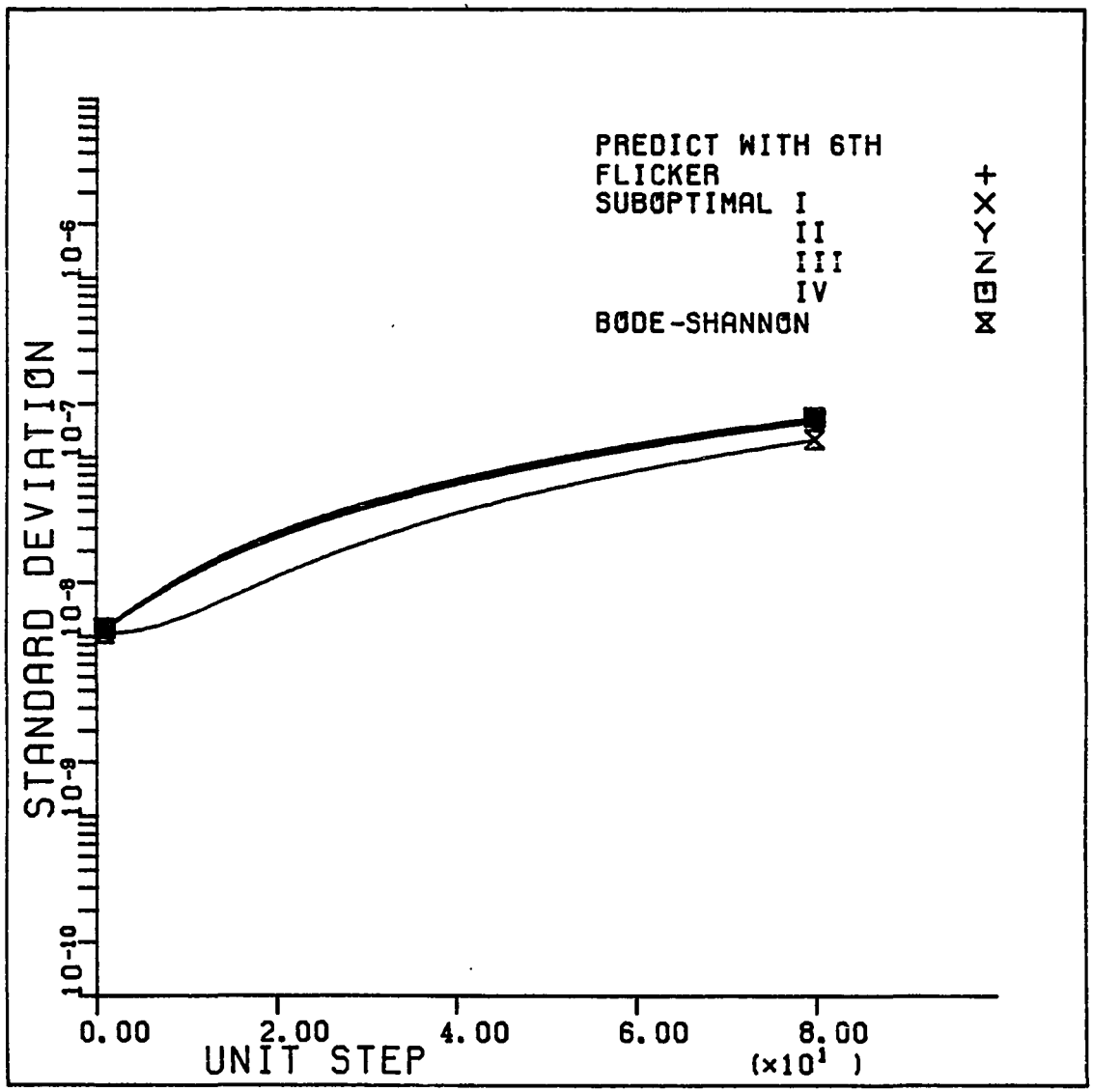

FIGURE 15. Suboptimal error analysis with 6th order model (prediction)

B. Application to the Global Positioning System

Our clock noise model can be applied to the Global Positioning System (GPS) [37,38] which enables a user to locate his or her position. In the GPS, users have ordinary quartz clocks which are less accurate than precision atomic clocks installed in the satellites. The user clock experiences some drift and develops clock bias with respect to a satellite clock. The clock bias introduces a positioning error in the user system.

To apply the developed clock model to the GPS, consider a stationary user case, for simplicity, in the earth centered inertial coordinate system as shown in Figure 16 [37].

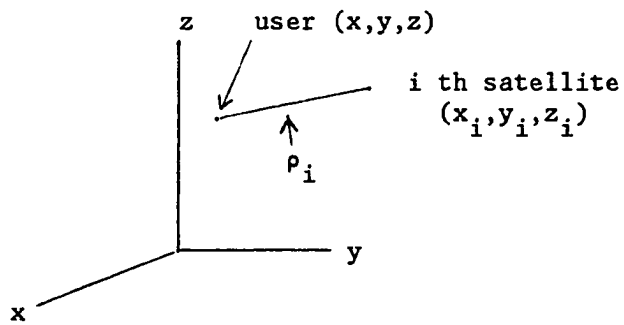

FIGURE 16. Earth centered coordinates

Let a user position be (x,y,z) and let t_b be a clock bias. Assign state variables x_i's to x, y, z, and t_b such that $x_1 = \Delta x$, $x_2 = \Delta y$, $x_3 = \Delta z$, and $x_4 = \Delta t_b$, where Δ is an increment from nominal values. Then,

the dynamics are given by the following equation.

$$\begin{bmatrix} \dot{x}_1 \\ \dot{x}_2 \\ \dot{x}_3 \\ \dot{x}_4 \\ \dot{x}_5 \\ \dot{x}_6 \\ \vdots \\ \dot{x}_{5+n} \end{bmatrix} = \begin{bmatrix} 0 & 0 & 0 & 0 & 0 & 0 & 0 & 0 \\ 0 & 0 & 0 & 0 & 0 & 0 & 0 & 0 \\ 0 & 0 & 0 & 0 & 0 & 0 & 0 & 0 \\ 0 & 0 & 0 & 0 & 1 & 1 & \cdots & 1 \\ 0 & 0 & 0 & 0 & 0 & 0 & \cdots & 0 \\ 0 & 0 & 0 & 0 & 0 & -\lambda_1 & \cdots & 0 \\ & & \vdots & & & & & \\ 0 & 0 & 0 & 0 & 0 & 0 & & -\lambda_n \end{bmatrix} \begin{bmatrix} x_1 \\ x_2 \\ x_3 \\ x_4 \\ x_5 \\ x_6 \\ \vdots \\ x_{5+n} \end{bmatrix} + \begin{bmatrix} w_x \\ w_y \\ w_z \\ w_0 \\ w_{-2} \\ K_1 w_{-1} \\ \vdots \\ K_n w_{-1} \end{bmatrix} \quad (5.12)$$

where w_x, w_y, and w_z are noises in the x, y, and z axis, respectively. In equation (5.12), the lower right of the system matrix is identical with that of equation (4.8) of the clock noise model.

Before setting up a Kalman filter equation, consider a measurement equation z_k. To do this, start from a range distance ρ_i in Figure 16.

$$\rho_i = [\ (x-x_i)^2 + (y-y_i)^2 + (z-z_i)^2\ ]^{1/2} + ct_b \quad (5.13)$$

where c is the velocity of light.

Let (x_0, y_0, z_0) be the nominal position and Δx, Δy, Δz be increments on the user position (x,y,z) from the (x_0, y_0, z_0), respectively. And let Δt_b be an increment on t_b from the nominal t_{b_0}.

Then, by linearizing equation (5.13), we get

$$\begin{bmatrix} \alpha_{x_1} & \alpha_{y_1} & \alpha_{z_1} & c \\ \alpha_{x_2} & \alpha_{y_2} & \alpha_{z_2} & c \\ \alpha_{x_3} & \alpha_{y_3} & \alpha_{z_3} & c \\ \alpha_{x_4} & \alpha_{y_4} & \alpha_{z_4} & c \end{bmatrix} \begin{bmatrix} \Delta x \\ \Delta y \\ \Delta z \\ \Delta t_b \end{bmatrix} = \begin{bmatrix} \Delta\rho_1 \\ \Delta\rho_2 \\ \Delta\rho_3 \\ \Delta\rho_4 \end{bmatrix} \tag{5.14}$$

where α_{x_i} is the direction cosine of the angle such that

$$\alpha_{x_i} = \frac{x-x_i}{\rho_i - ct_b}$$

With this fact, we have the following Kalman filter parameters with time step size Δt.

State transition matrix Φ is given by

$$\Phi = \left[\begin{array}{ccc|c} 1 & 0 & 0 & \\ 0 & 1 & 0 & 0 \\ 0 & 0 & 1 & \\ \hline & 0 & & \text{from eq. (4.12)} \\ & & & \text{with } t = \Delta t \end{array}\right] \tag{5.15}$$

Q matrix is given by

$$Q_k = \left[\begin{array}{ccc|c} S_x & 0 & 0 & \\ 0 & S_y & 0 & 0 \\ 0 & 0 & S_z & \\ \hline & 0 & & \text{from eq. (4.31)} \end{array}\right] \tag{5.16}$$

where S_x, S_y, and S_z are spectral amplitudes of x, y, and z axis noises, respectively.

H matrix is determined from equation (5.14).

$$H = \begin{bmatrix} \alpha_{x_1} & \alpha_{y_1} & \alpha_{z_1} & c & 0 & \cdots & 0 \\ \alpha_{x_2} & \alpha_{y_2} & \alpha_{z_2} & c & 0 & \cdots & 0 \\ \alpha_{x_3} & \alpha_{y_3} & \alpha_{z_3} & c & 0 & \cdots & 0 \\ \alpha_{x_4} & \alpha_{y_4} & \alpha_{z_4} & c & 0 & \cdots & 0 \end{bmatrix} \tag{5.17}$$

Initial conditions are as follows:

$$\underline{\hat{x}}_0^- = [\, x_0 \quad y_0 \quad z_0 \quad t_{b_0} \quad 0 \quad \cdots \quad 0 \,]^T \tag{5.18}$$

$$P_0^- = \underline{0} \tag{5.19}$$

We can use the results obtained in Chapter IV to compute the Φ and Q matrices in equations (5.15) and (5.16).

In this section, we have shown that the state modeling of clock noises is imbedded into the Global Positioning System. The simplification used in the truth and suboptimal models is sufficient for describing the $\frac{1}{f}$ noise in the GPS application.

VI. CONCLUSION

In this paper, state model of clock noises and corresponding Kalman filter mechanization have been studied. The clock noise is typically expressed as a sum of the three noise processes - white, flicker, and random-walk noises. Among these three, our main concern is how to implement the flicker noise process, since it involves the realization of a shaping filter which is best described by an irrational transfer function $\frac{1}{\sqrt{s}}$.

It is shown that $\frac{1}{\sqrt{s}}$ can be approximated with a rational function in s by using the continued fraction expansion method. With an aid of this method, the rational approximations $\{R_n(s)\}_{n=1}^{\infty}$ are sequentially generated, whereas other methods such as least square approximations require the solution of nonlinear equations for the optimization. Steiglitz's method [18] discussed in Chapter III can be considered as a special case of the proposed method. The rational approximations were realized in this analysis with a bank of parallel first-order filters.

In $\{R_n(s)\}$, the numerator and denominator of $R_n(s)$ are Hurwitz polynomials. Furthermore, $R_n(s)$ is stable and has a minimal phase. Poles and zeros of $R_n(s)$ are located on the negative real axis which is a branch cut of $\frac{1}{\sqrt{s}}$. The poles of $R_{2n-1}(s)$ are more widely dispersed than those of $R_{2n}(s)$ and thus it is a little simpler to implement and preferable to get a good approximation over a wider frequency range.

When n is even, $R_n(s)$ is proper. When n odd, $R_n(s)$ is strictly proper. In the use of $\{R_n(s)\}$, the size of n can be chosen relatively small, if $R_n(s)$ covers only few decades of the frequency or time interval. The realization of $R_n(s)$ is controllable and observable.

Based upon this approximation, i.e., $R_{2n-1}(s)$ plus the white and random-walk noises, the Kalman filter equations for the clock noise model were constructed in Chapter IV. To assess the clock error propagation with time, the error analysis was performed. A simplified 2-state suboptimal filter was run in parallel with a truth model Kalman filter of dimension (n+2) for the comparison study. In case of the clock error prediction, the optimum prediction error and optimum error predictor were analytically obtained by using the Bode-Shannon method. The optimum prediction error formula coincides with Q_{11} of the truth model Q matrix, and it was compared with prediction errors obtained from the Kalman filters. The optimum prediction error clearly yields a smaller increase when compared to the truth or 2-state suboptimal models, as time passes. At $t = 80$ steps, with step size $\Delta t = 1$, the Kalman filter prediction estimates become 30% larger than the optimal estimate, which could be too large in some applications.

It shows that for a long-term behavior ($t \geq 1$), the random-walk noise component dominates the other two noise processes. This agrees with the fact, mentioned in Chapter II, that the random-walk noise is more divergent than the flicker noise process. Hence, the effect of the flicker noise is negligible for the long-range estimation and prediction of the clock error in the 2-state suboptimal filter. This suggests how

to pick a Q matrix in the 2-state suboptimal filter. A simple choice of the Q matrix for the 2-state suboptimal model is just to take most upper left (2×2) submatrix of the already developed higher-order truth model Q matrix.

Many researchers have tried to imbed the effect of the flicker noise process into the Q matrix in the suboptimal filter, even though there is no flicker noise component in the suboptimal filter. From the comparison study, it was found that the Q matrix in the 2-state model can be prescribed by only considering the white and random-walk noise processes without degrading the overall performance much. It was also found that the Q matrix parameters were not especially critical for both the filter and predictive estimators.

The truth and suboptimal models with appropriate Q matrices can be applied to the GPS user receiver systems as discussed briefly in Chapter V and to any precise clock system.

VII. FURTHER STUDY

1. As one of the author's committee members pointed out, study on a time series of clock error due to real clock noise is needed. It can be carried out with a spectrum of the time series. From the time series, the flicker (1/f noise) portion of a spectrum of data can be obtained and studied. By doing so, a good comparison of the developed model of 1/f noise with real clock noise may be obtained.

2. Study between the continued fraction expansion method and other methods briefly discussed in Chapter III is needed in various ranges of frequency.

3. The developed clock model must be tested in real situations with various cases, i.e., satellite failures, coarse clock systems, and so on.

VIII. BIBLIOGRAPHY

1. James A. Barnes, A. R. Chi, L.S. Cutler, D. J. Healy, D. B. Leason, T. E. McGunigal, J. A. Mullen, Jr., W. L. Smith, R. L. Sydnor, R. F. C. Vessot, and G. M. R. Winkler. "Characterization of Frequency Stability". IEEE Transactions Instrument and Measurement, 20, No. 2 (May 1971), 105-120.

2. E. Parzen. Stochastic Process. San Francisco: Holden-Day, Inc., 1962.

3. R. Grover Brown. Introduction to Random Signal Analysis and Kalman Filtering. New York: John Wiley & Sons, Inc., 1983.

4. A. van der Ziel. "Flicker Noise in Electron Devices". In Advances in Electron and Physics. Vol. 49. New York: Academic Press, 1979, pp. 225-297.

5. R. F. Voss and J. Clarke. "1/f Noise in Music: Music from 1/f Noise". Journal of Acoustics Society of America, 63, No. 1 (Jan. 1978), 258-263.

6. D. Brouwer. "A Study of the Changes in the Rate of Rotation of the Earth". Astronomical Journal, 57, No. 5 (Sept. 1952), 125-146.

7. D. W. Allan. "Statistics of Atomic Frequency Standards". Proc. of IEEE, 54, No. 2 (Feb. 1966), 221-230.

8. J. A. Barnes. "Models for the Interpretation of Frequency Stability Measurements". NBS Technical Note, No. 683 (Aug. 1976).

9. M. J. Buckingham. Noise in Electron Devices and Systems. Chichester, England: Ellis Horwood Ltd., 1983.

10. M. A. Caloyanides. "Microcycle Spectral Estimates of 1/f Noise in Semiconductors". Journal of Applied Physics, 45, No. 1 (Jan. 1974), 307-316.

11. I. Flinn. "Extent of the 1/f Noise Spectrum". Nature, 219, No. 5161 (Sept. 28, 1968), 1356-1357.

12. N. N. Lebedev. Special Functions and Their Applications. Englewood Cliffs, N.J.: Prentice-Hall, Inc., 1965.

13. V. Redeka. "1/f Noise in Physical Measurements". IEEE Transactions Nuclear Science, 16 (Oct. 1969), 17-35.

14. D. Halford. "A General Mechanical Model for $|f|^{\alpha}$ Spectral Density Random Noise with Special Reference to Flicker Noise $1/|f|$". Proc.

of IEEE, 56, No. 3 (Mar. 1968), 251-258.

15. K. Oldham. "Semiintegral Electroanalysis: Analog Implementation". Analytical Chemistry, 45, No. 1 (Jan. 1973), 39-46.

16. C. Maccone. "$1/f^x$ Noises and the Riemann-Liouville Fractional Integral/Derivative of the Brownian Motion". In 6th International Conference on Noise in Physical Systems Proceeding, NBS Special Publication, No. 614 (1981), 192-195.

17. D. A. Bell. Noise and the Solid State. Plymouth, London: Pentech Press, 1985.

18. C. T. Chen. Introduction to Linear System Theory. New York: Holt, Rinehart and Winston, Inc., 1970.

19. J. H. Laning, Jr. and R. H. Battin. Random Processes in Automatic Control. New York: McGraw-Hill, 1956.

20. K. Steiglitz. "An RC Impedance Approximants to $s^{-1/2}$ ". IEEE Transaction Circuit Theory, 11, No. 1 (March 1964), 160-161.

21. A. N. Khovanskii. The Application of Continued Fractions and Their Generalizations to Problems in Approximation Theory. Gronigen, Netherlands: P. Noordhoff, Ltd., 1963.

22. H. S. Wall. Analytic Theory of Continued Fractions. New York: Academic Press, 1975.

23. G. A. Baker, Jr. Essentials of Pade Approximants. New York: Academic Press, 1975.

24. A. Bultheel. "Applications of Pade Approximants and Continued Fractions in System Theory". In Mathematical Theory of Networks and Systems. Ed. P. A. Fuhrmann. New York: Springer-Verlag, 1984, pp. 130-148.

25. N. K. Bose. "Properties of Pade Approximants to Stieltjes Series and Systems Theory". In Lecture Notes in Mathematics 1105, Rational Approximation and Interpolation. New York: Springer-Verlag, 1984, pp. 182-188.

26. J. C. Mason. "Some Applications and Drawbacks of Pade Approximants". In Approximation Theory and Applications. Ed. Z. Ziegler. New York: Academic Press, 1981.

27. T. E. Fortmann. "A Matrix Inversion Identity". IEEE Transactions Automatic Control, 15, No. 5 (Oct. 1970), 599.

28. R. S. Bucy and P. D. Joseph. Filtering for Stochastic Processes

with Applications to Guidance. New York: Interscience, 1968.

29. H. W. Sorenson. "Kalman Filtering Techniques". In Advances in Control Systems. Vol. 3. Ed. C. T. Leondes. New York: Academic Press, 1966.

30. P. S. Maybeck. Stochastic Models, Estimation, and Control. Vol. 1. New York: Academic Press, 1979.

31. A. J. van Dierendonck, J. B. McGraw, and R. G. Brown. "Relationship between Allan Variances and Kalman Filter Parameters". Proceedings of the Sixteenth Annual Precise Time and Time Interval (PTTI) Applications and Planning Meeting, (Nov. 1984), pp. 273-293.

32. J. S. Meditch. Stochastic Optimal Linear Estimation and Control. New York: McGraw-Hill, 1969.

33. H. W. Bode and C. E. Shannon. "A Simplified Derivation of Linear Least Square Smoothing and Prediction Theory". Proc. of IRE, 38 (April 1950), 417-425.

34. R. G. Brown and J. W. Nilsson. Introduction to Linear Systems Analysis. New York: John Wiley and Sons, Inc., 1962.

35. C. Moler and C. V. Loan. "Nineteen Dubious Ways to Compute the Exponential of a Matrix". SIAM Review, 20, No. 4 (Oct. 1978), 801-836.

36. A. J. van Dierendonck, and Q. D. Hua. "Enhancements to the TTS-502 Time Transfer System". Proceedings of the Fifteenth Annual Precise Time and Time Interval (PTTI) Applications and Planning Meeting, (Dec. 1983), pp. 133-154.

37. P.S. Jorgensen. "Navstar/Global Positioning System 18 Satellite Constellations". Navigation, Journal of ION, 27, No. 2 (Summer 1983), 89-100.

38. M. A. Sturza. "GPS Navigation Using Three Satellites and a Precise Clock". Navigation, Journal of ION, 30, No. 2 (Summer 1983), 146-155.

IX. ACKNOWLEDGEMENT

I wish to express my gratitude to those who helped make this research possible.

First of all, I would like to express my deep appreciation to Dr. Robert Grover Brown, major advisor, for his endless help and guidance. His knowledge and insight were crucial in leading me to the right direction.

Secondly, many thanks are due to my committee members, Dr. T. M. Scott, Dr. J. P. Basart, Dr. H. C. Hsieh, and Dr. R. J. Lambert for their helpful suggestions and criticisms.

Special thanks go to the Department of Electrical Engineering and Computer Engineering, and the Graduate College of Iowa State University for needed financial support throughout my research.

Last, but not least, I thank my wife, Eunlee, and son, Stephen Sejin, for their constant encouragement and understanding at home, while I pursued an advanced degree. It would have been very difficult without their support.

X. APPENDIX

The following listings illustrate sample error analysis programs for the 5th order and 2-state suboptimal models. In the program, the Simplotter subroutine is used for plotting.

This is an estimation portion of the error analysis program.

```
//ESTMATE5 JOB I6954,AHN
//STEP1 EXEC FORTGS
//FORT.SYSIN  DD  *
      DOUBLE PRECISION TIME,T,SUM,SUMT,E1,E2,FS,FT,PHIS,PHIT,HS,HT,
     1                 QS,QT,RS,RT,GS,GT,GO,PNS,PNT,PNO,TSTEP,
     2                 PPS,PPT,PPO,HPRS,HPRO,HG,RGT,SDPPO,SDPPT1,
     3                 SDPPT2,SDPPT3,SDPPT4,ERROR,ESUM,PRDERR
      DIMENSION E1(5,5),E2(5,5),FS(2,2),FT(5,5),PHIS(2,2),PHIT(5,5),
     1          HS(2),HT(5),QS(2,2),QT(5,5),TSTEP(280),SDPPO(280),
     2          GS(2),GT(5),GO(5),PNS(2,2),PNT(5,5),PNO(5,5),PPS(2,2),
     3          PPT(5,5),PPO(5,5),HG(5,5),RGT(5,5),PRDERR(290),
     4          SDPPT1(280),SDPPT2(280),SDPPT3(280),SDPPT4(280)
C     ------------------------------------------------------------
C     T=TRUTH MODEL,  S=SUBOPTIMAL MODEL,  O=OPTIMAL
C     ------------------------------------------------------------
C     GET THE INITIAL DATA.
      NO=5
      NT=5
      NS=2
      TIME=1.D0
      ISTEP1=50
      ISTEP2=70
      ISTEP3=170
C     ----------------------------------------
C     INITIALIZE THE IDENTITY MATRIX.
      DO 500 I=1,NT
         DO 500 J=1,NT
            E1(I,J)=0.D0
500         E1(I,I)=1.D0
C     ----------------------------------------------
C     READ THE INPUT MATRICES.
C     READ THE SYSTEM MATRIX OF SUBOPTIMAL SYSTEM.
      DO 510 I=1,NS
510     READ(5,550) (FS(I,J),J=1,NS)
C
C     READ THE STATE TRANSITION MATRIX OF SUBOPTIMAL SYSTEM.
      DO 520 I=1,NS
```

```
520     READ(5,550) (PHIS(I,J),J=1,NS)
C
C     READ THE H AND R MATRICES OF SUBOPTIMAL SYSTEM.
      READ(5,550) (HS(I),I=1,NS),RS
550   FORMAT(4D16.7)
C
C     ---------------------------------------------------
C     READ THE SYSTEM MATRIX OF THE TRUTH MODEL.
      DO 560 I=1,NT
560     READ(5,550) (FT(I,J),J=1,NT)
C
C     READ THE STATE TRANSITION MATRIX OF THE TRUTH MODEL.
      DO 565 I=1,NT
565     READ(5,550) (PHIT(I,J),J=1,NT)
C
C     READ THE Q-SUBMATRIX OF THE TRUTH MODEL.
      DO 580 I=1,NT
580     READ(5,550) (QT(I,J),J=1,NT)
C
C
C     READ THE H AND R OF THE TRUTH MODEL.
         READ(5,550) (HT(I),I=1,NT)
         READ(5,550) RT
C     ---------------------------------------
      DO 1600 IQ=1,4
C      READ Q-MATRICES OF SUBOPTIMAL SYSTEMS.
       DO 600 I=1,NS
600       READ(5,550) (QS(I,J),J=1,NS)
C
C     SET A PRIORI COV OF SUBOPTIMAL SYSTEM TO ZERO.
      DO 620 I=1,NS
         DO 620 J=1,NS
620         PNS(I,J)=0.D0
C
C     SET A PRIORI COV. MATRIX OF THE TRUTH MODEL TO ZERO.
      DO 630 I=1,NT
         DO 630 J=1,NT
            PNT(I,J)=0.D0
C     GET THE INITIAL A PRIORI ERROR COV FROM THE TRUTH MODEL.
630         PNO(I,J)=0.D0
C     ---------------------------------------
C     WRITE THE DATA OF THE KALMAN FILTER PARAMETERS.
C
      WRITE(6,750)
750   FORMAT(1H0,'SUBOPTIMAL SYSTEM ------------------------------')
      WRITE(6,751)
751   FORMAT(1H ,'SYSTEM MATRIX',12X,'STATE TRANSITION MATRIX')
      DO 752 I=1,NS
752     WRITE(6,850) (FS(I,J),J=1,NS),(PHIS(I,J),J=1,NS)
C
```

```
      WRITE(6,753)
753   FORMAT(1HO,'MEAS.  MATRIX',12X,'MEAS. ERROR COV. R')
      WRITE(6,850) (HS(I),I=1,NS),RS
      WRITE(6,756)
756   FORMAT(1HO,'A PRIORI ERROR COVARIANCE',1X,'Q-MATRIX')
      DO 758 I=1,NS
758     WRITE(6,850) (PNS(I,J),J=1,NS),(QS(I,J),J=1,NS)
C
850   FORMAT(1H ,10(D12.4,1X))
C
C
      WRITE(6,852)
852   FORMAT(1HO,'TRUTH MODEL----------------------------------------')
      WRITE(6,853)
853   FORMAT(1H ,'SYSTEM MATRIX',52X,'STATE TRANSITION MATRIX')
      DO 854 I=1,NT
854     WRITE(6,850) (FT(I,J),J=1,NT),(PHIT(I,J),J=1,NT)
      WRITE(6,856)
856   FORMAT(1HO,'MEAS.  MATRIX',52X,'MEAS. ERROR COV. R')
      WRITE(6,850) (HT(I),I=1,NT),RT
      WRITE(6,857)
857   FORMAT(1HO,'A PRIORI ERROR COVARIANCE',40X,'Q-MATRIX')
      DO 858 I=1,NT
858     WRITE(6,850) (PNT(I,J),J=1,NT),(QT(I,J),J=1,NT)
C
C
C     ------------------------------------------------------
C
      DO 1600 K=1,ISTEP3
C
C     COMPUTE THE GAINS OF THE SUBOPTIMAL AND THE TRUTH MODELS.
C
C     COMPUTE THE SUBOPTIMAL GAINS GS.
      SUM=0.DO
      DO 1110 M1=1,NS
         DO 1110 M2=1,NS
1110        SUM=SUM+HS(M1)*PNS(M1,M2)*HS(M2)
C
      HPRS=(SUM+RS)
C
      DO 1130 I=1,NS
         SUM=0.DO
         DO 1120 M1=1,NS
1120        SUM=SUM+PNS(I,M1)*HS(M1)
1130     GS(I)=SUM/HPRS
C     ----------------------------------------
C     COMPUTE THE OPTIMAL GAINS GO OF THE TRUTH MODEL.
      SUM=0.DO
      DO 1160 M1=1,NO
         DO 1160 M2=1,NO
```

```
1160        SUM=SUM+HT(M1)*PNO(M1,M2)*HT(M2)
C
      HPRO=(SUM+RT)
C
      DO 1180 I=1,NO
         SUM=0.D0
         DO 1170 M1=1,NO
1170        SUM=SUM+PNO(I,M1)*HT(M1)
1180     GO(I)=SUM/HPRO
C     ------------------------------------
C     UPDATE THE COVARIANCES.
C
C     UPDATE THE COV. OF THE SUBOPTIMAL SYSTEM.
      DO 1210 I=1,NS
         DO 1210 J=1,NS
            HG(I,J)=GS(I)*HS(J)
1210        E2(I,J)=E1(I,J)-HG(I,J)
C
      DO 1230 I=1,NS
         DO 1230 J=1,NS
            SUM=0.D0
            DO 1220 M1=1,NS
1220           SUM=SUM+E2(I,M1)*PNS(M1,J)
1230        PPS(I,J)=SUM
C     ------------------------------------------------
C     PLUG THE SUBOPTIMAL GAINS INTO THE TRUTH MODEL.
C
      DO 1240 I=1,NS
1240     GT(I)=GS(I)
C
      L=NS+1
      IF (L.GE.NT) GOTO 1270
      DO 1250 I=L,NT
1250     GT(I)=0.D0
C     ----------------------------
C     COMPUTE THE COV. OF THE TRUTH MODEL WITH THE SUBOPTIMAL GAINS.
C
1270  DO 1280 I=1,NT
         DO 1280 J=1,NT
            HG(I,J)=GT(I)*HT(J)
            E2(I,J)=E1(I,J)-HG(I,J)
1280        RGT(I,J)=GT(I)*RT*GT(J)
C
      DO 1300 I=1,NT
         DO 1300 J=1,NT
         SUM=0.D0
         DO 1290 M1=1,NT
            DO 1290 M2=1,NT
1290           SUM=SUM+E2(I,M1)*PNT(M1,M2)*E2(J,M2)
1300     PPT(I,J)=SUM+RGT(I,J)
```

```
C     ------------------------------------------------------
C     UPDATE THE COV. OF THE TRUTH MODEL WITH OPTIMAL GAINS.
C
      DO 1310 I=1,NO
         DO 1310 J=1,NO
            HG(I,J)=GO(I)*HT(J)
1310        E2(I,J)=E1(I,J)-HG(I,J)
C
      DO 1330 I=1,NO
         DO 1330 J=1,NO
            SUM=0.DO
            DO 1320 M1=1,NO
1320           SUM=SUM+E2(I,M1)*PNO(M1,J)
1330        PPO(I,J)=SUM
C     ------------------------------------
C     PROJECT AHEAD OF THE COV. OF THE SUBOPTIMAL SYSTEM.
C
      DO 1360 I=1,NS
         DO 1360 J=1,NS
            SUM=0.DO
            DO 1350 M1=1,NS
               DO 1350 M2=1,NS
1350              SUM=SUM+PHIS(I,M1)*PPS(M1,M2)*PHIS(J,M2)
1360        PNS(I,J)=SUM+QS(I,J)
C     ------------------------------------
C     PROJECT AHEAD OF COV. OF THE TRUTH MODEL WITH SUBOPTIMAL GAINS.
C
      DO 1400 I=1,NT
         DO 1400 J=1,NT
            SUM=0.DO
            DO 1380 M1=1,NT
               DO 1380 M2=1,NT
1380              SUM=SUM+PHIT(I,M1)*PPT(M1,M2)*PHIT(J,M2)
1400        PNT(I,J)=SUM+QT(I,J)
C     ------------------------------------
C     PROJECT AHEAD OF THE COV. OF THE TRUTH MODEL WITH OPTIMAL GAINS.
C
      DO 1440 I=1,NO
         DO 1440 J=1,NO
            SUM=0.DO
            DO 1420 M1=1,NO
               DO 1420 M2=1,NO
1420              SUM=SUM+PHIT(I,M1)*PPO(M1,M2)*PHIT(J,M2)
1440        PNO(I,J)=SUM+QT(I,J)
C     ------------------------------------------------
C     CALCULATE THE STANDARD DEVIATIONS OF A POSTERIORI ERROR COV.
      IF (IQ.EQ.1) SDPPT1(K)=DSQRT(PPT(1,1))/TIME
      IF (IQ.EQ.2) SDPPT2(K)=DSQRT(PPT(1,1))/TIME
      IF (IQ.EQ.3) SDPPT3(K)=DSQRT(PPT(1,1))/TIME
      IF (IQ.EQ.4) SDPPT4(K)=DSQRT(PPT(1,1))/TIME
```

```
      SDPPO(K)=DSQRT(PPO(1,1))/TIME
C
C     TO FILTER THE PROCESS SET THE MEASUREMENT TO RT=RS=.5D-17.
      IF (K.NE.ISTEP1) GO TO 1595
         RT=6.25D-16
         RS=RT
C
C     TO PREDICT N STEPS AHEAD SET RT=RS=1.D0.
1595  IF (K.NE.ISTEP2) GO TO 1600
      RT=1.D0
      RS=RT
C     TO PREDICT I TIME UNITS AHEAD FIX ERROR=PPO(1,1) AT THE 70TH STEP.
         ERROR=PPO(1,1)
C
C
1600  CONTINUE
C     ------------------------------------------------------------
C     COMPUTE OPTIMAL PREDICTION OF I TIME UNITS AHEAD.
      DO 1610 I=ISTEP2,ISTEP3
         T=(I-ISTEP2)*TIME
         ESUM=4.715D-20*T + 3.6D-19*T*T + 2.50029D-20*T*T*T + ERROR
1610     PRDERR(I)=DSQRT(ESUM)/TIME
C
C
C     WRITE STANDARD DEVIATIONS OF SUBOPTIMAL PPT AND TRUTH PPO.
      WRITE(6,1620)
1620  FORMAT(1H1,'OPTIMAL STD',14X,'SUBOPTIMAL STANDARD DEVIATION')
      DO 1640 K=1,ISTEP3
1640     WRITE(6,1650) K,SDPPO(K),SDPPT1(K),SDPPT2(K),SDPPT3(K),
     1                 SDPPT4(K),PRDERR(K)
1650     FORMAT(1H ,I3,3X,6(D9.3,3X))
C
      DO 1800 K=2,ISTEP3
         TSTEP(K)=K*TIME
         SDPPO(K)=DLOG10(SDPPO(K))
         SDPPT1(K)=DLOG10(SDPPT1(K))
         SDPPT2(K)=DLOG10(SDPPT2(K))
         SDPPT3(K)=DLOG10(SDPPT3(K))
         SDPPT4(K)=DLOG10(SDPPT4(K))
         IF (K.LT.ISTEP2) GOTO 1800
         PRDERR(K)=DLOG10(PRDERR(K))
1800  CONTINUE
C
C     PLOT STANDARD DEVIATIONS OF THE ABOVE.
      KSTEP=-ISTEP3
      CALL GRAPH(KSTEP,TSTEP,SDPPO,103,102,5.0,-5.0,40.0,0.0,
     1           5.0,-10.0,'UNIT STEP;','STANDARD DEVIATION;',
     2          'FILTERING WITH 5TH;','FLICKER;')
      CALL GRAPHS(KSTEP,TSTEP,SDPPT1,204,102,'SUBOPTIMAL I;')
      CALL GRAPHS(KSTEP,TSTEP,SDPPT2,209,102,'           II;')
```

```
      CALL GRAPHS(KSTEP,TSTEP,SDFPT3,208,102,'          III;')
      CALL GRAPHS(KSTEP,TSTEP,SDPPT4,210,102,'          IV;')
C
      STOP
      END
//GO.SYSIN DD *
   0.0              0.1000000D 01
   0.0              0.0
   0.1000000D 01    0.1000000D 01
   0.0              0.1000000D 01
   0.1000000D 01    0.0              0.1000000D 01
   0.0              0.1000000D 01    0.1000000D 01    0.1000000D 01
   0.1000000D 01
   0.0              0.0              0.0              0.0
   0.0
   0.0              0.0             -0.7179670D-01    0.0
   0.0
   0.0              0.0              0.0             -0.1000000D 01
   0.0
   0.0              0.0              0.0              0.0
  -0.1392820D 02
   0.1000000D 01    0.1000000D 01    0.9649456D 00    0.6321206D 00
   0.7179672D-01
   0.0              0.1000000D 01    0.0              0.0
   0.0
   0.0              0.0              0.9307201D 00    0.0
   0.0
   0.0              0.0              0.0              0.3678794D 00
   0.0
   0.0              0.0              0.0              0.0
   0.8934257D-06
   0.4306232D-18    0.3746699D-19    0.1453159D-18    0.1610753D-18
   0.5026500D-19
   0.3746699D-19    0.7500899D-19    0.0              0.0
   0.0
   0.1453159D-18    0.0              0.6723979D-19    0.8268107D-19
   0.7231092D-19
   0.1610753D-18    0.0              0.8268107D-19    0.1087655D-18
   0.1266038D-18
   0.5026500D-19    0.0              0.7231092D-19    0.1266038D-18
   0.5096864D-18
   0.1000000D 01    0.0              0.0              0.0
   0.0
   0.1000000D 01
   0.4306000D-18    0.3747000D-19
   0.3747000D-19    0.7501000D-19
   0.7215000D-19    0.3747000D-19
   0.3747000D-19    0.7501000D-19
   0.4322000D-18    0.3975000D-18
   0.3975000D-18    0.5072000D-18
```

```
     0.4322000D-18    0.3975000D-18
     0.3975000D-18    0.7501000D-19
          STOP
          END
//
```

This is a prediction portion of the error analysis program.

```
//PRDCT5 JOB I6954,AHN
//S1 EXEC WATFIVS
//GO.SYSIN  DD  *
$JOB           AHN
      DOUBLE PRECISION PHIT,PHIS,QT,QS1,QS2,QS3,QS4,PT,PS1,PS2,PS3,PS4,
     1    K,RD,SUM,PI,H0,H1,H2,PRDCT,PRD1,PRD2,PRD3,PRD4,BD,SDPT,SDPS1,
     2    SDPS2,SDPS3,SDPS4,A,B,C,BB,CC,RDN,TSTEP
      DIMENSION PHIT(5,5),PHIS(2,2),QT(5,5),QS1(2,2),QS2(2,2),QS3(2,2),
     1    QS4(2,2),PT(5,5),PS1(2,2),PS2(2,2),PS3(2,2),PS4(2,2),K(3),
     2    RD(3),PRDCT(5,5),PRD1(5,5),PRD2(5,5),PRD3(5,5),PRD4(5,5),
     3    BD(100),SDPT(100),SDPS1(100),SDPS2(100),SDPS3(100),
     4    SDPS4(100),TSTEP(100)
C
C     INITIALIZE THE DATA.
C
      PI=3.141592D0
      NS=2
      NT=5
      NSTEP=80
      H0=9.43D-20
      H1=1.8D-19
      H2=3.8D-21
C
      K(1)=3.57265D-1
      K(2)=2.D0/3.D0
      K(3)=4.97607D0
C
      RD(1)=7.17967D-2
      RD(2)=2.D0/3.D0
      RD(3)=13.9282D0
C
      DO 1700 I=1,NT
1700     READ(5,1750) (PT(I,J),J=1,NT)
1750  FORMAT(4D16.7)
C
      DO 1800 I=1,NS
         DO 1800 J=1,NS
            PS1(1,1)=PT(1,1)
            PS1(1,2)=PT(1,2)
            PS1(2,1)=PT(2,1)
            PS1(2,2)=PT(2,2)
C
            PS2(1,1)=PT(1,1)
            PS2(1,2)=PT(1,2)
            PS2(2,1)=PT(2,1)
            PS2(2,2)=PT(2,2)
C
```

```
            PS3(1,1)=PT(1,1)
            PS3(1,2)=PT(1,2)
            PS3(2,1)=PT(2,1)
            PS3(2,2)=PT(2,2)
C
            PS4(1,1)=PT(1,1)
            PS4(1,2)=PT(1,2)
            PS4(2,1)=PT(2,1)
            PS4(2,2)=PT(2,2)
1800  CONTINUE
C
      DO 2000 I=1,NT
         DO 2000 J=1,NT
            QT(I,J)=0.D0
            PHIT(I,J)=0.D0
2000  CONTINUE
C
      PHIS(1,1)=1.D0
      PHIS(2,1)=0.D0
      PHIS(2,2)=1.D0
      PHIT(1,1)=1.D0
      PHIT(2,2)=1.D0
C
C     PREDICT UP TO NSTEPS AHEAD.
C
      DO 6000 N=1,NSTEP
         PHIT(1,2)=N
         PHIS(1,2)=N
         DO 3100 J=1,3
            JJ=J+NS
C           TO AVOID UNDERFLOW TEST ARGUMENT OF DEXP FUNCTION.
            RDN=RD(J)*N
C
            IF (RDN.GT. 25.D0) THEN DO
               PHIT(JJ,JJ)=0.D0
             ELSE DO
               PHIT(JJ,JJ)=-DEXP(-RDN)
             END IF
C
            PHIT(1,JJ)=(1.D0+PHIT(JJ,JJ))/RD(J)
3100     CONTINUE
C
C
C        FIRST CANDIDATE OF Q-SUBOP.
         QS1(1,1)=H0*N/2.D0+2.D0*H1*N**2+2.D0*PI**2/3.D0*H2*N**3
         QS1(1,2)=PI**2*H2*N**2
         QS1(2,1)=QS1(1,2)
         QS1(2,2)=2.D0*PI**2*H2*N
C
C        SECOND CANDIDATE OF Q-SUBOP.
```

```
      QS2(1,1)=H0*N/2.D0+2.D0*PI**2/3.D0*H2*N**3
      QS2(1,2)=QS1(1,2)
      QS2(2,1)=QS2(1,2)
      QS2(2,2)=QS1(2,2)
C
C     THIRD CANDIDATE OF Q-SUBOP.
      QS3(1,1)=QS1(1,1)
      QS3(1,2)=2.D0*H1*N+PI**2*H2*N**2
      QS3(2,1)=QS3(1,2)
      QS3(2,2)=H0/(2.D0*N)+2.D0*H1+8.D0/3.D0*PI**2*N
C
C     FOURTH CANDIDATE OF Q-SUBOP.
      QS4(1,1)=QS1(1,1)
      QS4(1,2)=QS3(1,2)
      QS4(2,1)=QS4(1,2)
      QS4(2,2)=QS1(2,2)
C
C     5TH ORDER Q MATRIX.
      QT(1,1)=QS1(1,1)
      QT(1,2)=QS1(1,2)
      QT(2,1)=QT(1,2)
      QT(2,2)=QS1(2,2)
C
      DO 3300 I=1,3
         DO 3300 J=1,3
            II=I+NS
            JJ=J+NS
            A=(RD(I)+RD(J))*N
C
            IF (A.LT. 25.D0) THEN DO
              QT(II,JJ)=K(I)*K(J)*(1.D0-DEXP(-A))/(RD(I)+RD(J))*PI*H1
             ELSE DO
              QT(II,JJ)=K(I)*K(J)/(RD(I)+RD(J))*PI*H1
            END IF
3300  CONTINUE
C
      DO 3600 J=1,3
         SUM=0.D0
         DO 3500 I=1,3
C
C              TO AVOID UNDERFLOW IN EXPONENTIAL FUNCTION TEST ARGUMENT.
               B=RD(J)*N
               IF (B.GT. 25.D0) THEN DO
                  BB=0.D0
               ELSE DO
                 BB=DEXP(-B)
               END IF
C
               C=(RD(J)+RD(I))*N
               IF (C.GT. 25.D0) THEN DO
```

```
                  CC=0.D0
                ELSE DO
                  CC=DEXP(-C)
                END IF
C
                SUM=SUM+((1.D0-BB)/RD(J)-(1.D0-CC)/(RD(I)+RD(J)))
     1               *K(J)*K(I)/RD(I)
3500          CONTINUE
              QT(1,J+NS)=SUM*PI*H1
3600       CONTINUE
C
C      COMPUTE PREDICTION ERROR OF THE FIRST CANDIDATE.
           DO 4200 I=1,NS
              DO 4200 J=1,NS
                 SUM=0.D0
                 DO 4000 M1=1,NS
                    DO 4000 M2=1,NS
                       SUM=SUM+PHIS(I,M1)*PS1(M1,M2)*PHIS(J,M2)
4000             CONTINUE
              PRD1(I,J)=SUM+QS1(I,J)
4200       CONTINUE
C
C      COMPUTE PREDICTION ERROR OF THE SECOND CANDIDATE.
           DO 4400 I=1,NS
              DO 4400 J=1,NS
                 SUM=0.D0
                 DO 4300 M1=1,NS
                    DO 4300 M2=1,NS
                       SUM=SUM+PHIS(I,M1)*PS2(M1,M2)*PHIS(J,M2)
4300             CONTINUE
              PRD2(I,J)=SUM+QS2(I,J)
4400       CONTINUE
C
C      COMPUTE PREDICTION ERROR OF THE THIRD CANDIDATE.
           DO 4600 I=1,NS
              DO 4600 J=1,NS
                 SUM=0.D0
                 DO 4500 M1=1,NS
                    DO 4500 M2=1,NS
                       SUM=SUM+PHIS(I,M1)*PS3(M1,M2)*PHIS(J,M2)
4500             CONTINUE
              PRD3(I,J)=SUM+QS3(I,J)
4600       CONTINUE
C
C      COMPUTE PREDICTION ERROR OF THE FOURTH CANDIDATE.
           DO 4800 I=1,NS
              DO 4800 J=1,NS
                 SUM=0.D0
                 DO 4700 M1=1,NS
                    DO 4700 M2=1,NS
```

```
                    SUM=SUM+PHIS(I,M1)*PS4(M1,M2)*PHIS(J,M2)
4700            CONTINUE
              PRD4(I,J)=SUM+QS4(I,J)
4800       CONTINUE
C
C       COMPUTE PREDICTION ERROR OF THE 5TH ORDER MODEL.
           DO 5000 I=1,NT
              DO 5000 J=1,NT
                 SUM=0.D0
                 DO 4900 M1=1,NT
                    DO 4900 M2=1,NT
                       SUM=SUM+PHIT(I,M1)*PT(M1,M2)*PHIT(J,M2)
4900             CONTINUE
                 PRDCT(I,J)=SUM+QT(I,J)
5000       CONTINUE
C
C       PREDICTION BY BODE-SHANNON METHOD.
           BD(N)=DSQRT(PT(1,1)+QS1(1,1))
           SDPT(N)=DSQRT(PRDCT(1,1))
           SDPS1(N)=DSQRT(PRD1(1,1))
           SDPS2(N)=DSQRT(PRD2(1,1))
           SDPS3(N)=DSQRT(PRD3(1,1))
           SDPS4(N)=DSQRT(PRD4(1,1))
C
       WRITE (6,5200) N,SDPT(N),SDPS1(N),SDPS2(N),SDPS3(N),SDPS4(N),BD(N)
5200   FORMAT(1H ,I3,3X,6(D15.7,3X))
6000   CONTINUE
C
       DO 7000 I=1,NSTEP
          TSTEP(I)=I*1.D0
          SDPT(I)=DLOG10(SDPT(I))
          SDPS1(I)=DLOG10(SDPS1(I))
          SDPS2(I)=DLOG10(SDPS2(I))
          SDPS3(I)=DLOG10(SDPS3(I))
          SDPS4(I)=DLOG10(SDPS4(I))
          BD(I)=DLOG10(BD(I))
7000   CONTINUE
C
C      PLOT STANDARD DEVIATIONS OF THE ABOVE.
       KSTEP=-NSTEP
       CALL GRAPH(KSTEP,TSTEP,SDPT,103,102,5.0,-5.0,20.0,0.0,
      1           5.0,-10.0,'UNIT STEP;','STANDARD DEVIATION;',
      2          'PREDICT WITH 5TH;','FLICKER;')
       CALL GRAPHS(KSTEP,TSTEP,SDPS1,204,102,'SUBOPTIMAL I;')
       CALL GRAPHS(KSTEP,TSTEP,SDPS2,209,102,'           II;')
       CALL GRAPHS(KSTEP,TSTEP,SDPS3,208,102,'           III;')
       CALL GRAPHS(KSTEP,TSTEP,SDPS4,210,102,'           IV;')
       CALL GRAPHS(KSTEP,TSTEP,BD,312,102,'BODE-SHANNON;')
       STOP
       END
```

```
$ENTRY
   0.1015599D-15   0.6944787D-17   0.1583614D-17   0.2850850D-18
   0.4209731D-19
   0.6944787D-17   0.1487705D-17  -0.2608252D-18  -0.6009047D-20
  -0.5585303D-21
   0.1583614D-17  -0.2608252D-18   0.4691109D-18   0.1244133D-18
   0.7218362D-19
   0.2850850D-18  -0.6009047D-20   0.1244133D-18   0.1256097D-18
   0.1265809D-18
   0.4209731D-19  -0.5585303D-21   0.7218362D-19   0.1265809D-18
   0.5096830D-18
/*
```